공학석사학위논문

Sequential Optimization of MCMC-based Indirect Measurement Locations for Accurate System Identification of Structures

구조물 물성치 MCMC 기반 간접 추정의 정확도 향상을 위한 관측 위치 순차적 최적화 기법

2019 년 2 월

서울대학교 대학원

건설환경공학부

유 승 민

Sequential Optimization of MCMC-based Indirect Measurement Locations for Accurate System Identification of Structures

구조물 물성치 MCMC 기반 간접 추정의 정확도 향상을 위한 관측 위치 순차적 최적화 기법

지도 교수 송 준 호

이 논문을 공학석사 학위논문으로 제출함

2019년 1월

서울대학교 대학원

건설환경공학부

유 승 민

유승민의 공학석사 학위논문을 인준함

2019년 1월

위 원 장 _____ (인)

부위원장 _____ (인)

위 원 _____ (인)

Abstract

Structures deteriorate naturally when they are used for a long time. Therefore, it is essential to accurately check the degree of deterioration of a structure in order to prevent accidents such as collapse. However, numerical values to detect the degree of deterioration such as the effective thickness are often difficult to measure directly. Thus, it is required to indirectly estimate values associated with deterioration by using direct observations such as strain or displacement obtained from a loading test. In this case, if the number of measurable direct observation is limited due to external factors, it is desirable to choose direct observation locations that can improve the accuracy of indirect estimations under a small number of direct observations.

This study proposes a sequential measurement location optimization method to improve the accuracy of an effective thickness indirect estimation of a structure when the number of strain observations is limited. For this goal, the effective thickness distribution of the structure is approximated first by using Karhunen-Loève expansion. Second, system identification based on Bayesian updating using Markov chain Monte Carlo simulation is performed to estimate mean and standard deviation of the effective thickness under given strain measurements. Third, three sequential direct observation selection methods are proposed using the estimated mean and standard deviation of the effective thickness. This study compares the accuracy of the sequentially selected observation locations with simultaneously selected observation locations by applied to the structure. The accuracy of the three sequential measurement location selection methods is also compared.

Through the proposed methods, it is possible to determine the next strain measurement location, which can effectively improve the accuracy of the effective thickness estimation, and can maximize the accuracy of the effective thickness estimation under a small number of strain observation locations. It is expected that the proposed methods can be applied to improve the accuracy of estimation of various properties related to the structural deterioration, which can be estimated indirectly.

Keyword: Structural deterioration, Effective thickness, Karhunen-Loève expansion, Markov chain Monte Carlo simulation, Bayesian updating, System Identification

Student Number: 2017-24757

Table of Contents

List of Figures

List of Tables

Chapter 1. Introduction

1.1. Research Background

A number of residential buildings in South Korea (hereafter, Korea) were built when the population grew rapidly in the 1960s and 1970s. Many of the residential buildings have already been demolished due to the implementation of reconstruction, but a considerable number of people still live in seemingly deteriorated apartments as shown in Figure 1.1. Other structures such as bridges are also often used in deteriorated condition. Furthermore, structures may deteriorate for a short use period because of fraudulent work.

Figure 1.1. Deteriorated apartment
(Gangnam Apartment, Gwanak-gu, Seoul, built in 1974)

Structures deteriorate naturally as the useable period becomes longer. If the deteriorated structure is not repaired or removed in advance, a lot of material damage and human fatality due to the destruction during use of the structure can happen. Therefore, it is essential to accurately evaluate the degree of deterioration of the structure in order to effectively manage the structure in use and to prevent unexpected accidents caused by damage or collapse of the structure.

However, numerical values such as the effective thickness that can detect the degree of deterioration, require a large amount of budget and time to directly measure using a non-destructive test. In addition, it is often difficult to directly measure the degree of deterioration due to the size and weight of the inspection equipment. Here, the effective thickness of the structure refers to the actual thickness of the structure excluding the portion where it cannot support the loads of the structure due to the corrosion of the steel or cracks in the concrete.

Therefore, it is required to indirectly estimate the deterioration of the structure by using direct observations such as strain and displacement obtained through a simple test. However, there are many cases in which the number of measureable values is limited due to various problems. In this context, it is also important to select observation locations that can obtain an estimated value which is close to the actual value and reduce the standard deviation of the estimated value under a small number of observations.

To indirectly estimate values related to deterioration, various methods have been proposed to predict the random field of unknown quantity. Karhunen-Loève expansion, Bayesian approach and Markov chain Monte Carlo (MCMC) have been proposed for a nonlinear system identification problem when an unknown quantity

is a random field (Kučerová & Sýkora, 2013; Lee & Song, 2017; Li, 2015; Mondal *et al.*, 2014). For example, Yi and Song (2018) estimated the effective thickness of a structure using the strain of the structure.

However, literature only suggests indirect estimation methods which use directly observed values at a predetermined location. There is a lack of research on the difference of system identification accuracy caused by location of direct observations. The results of system identification using MCMC involves an error with the actual value and the standard deviation of the results. These values also vary according to the observed location of the actual values. Therefore, additional research is needed to maximize the accuracy of system identification with MCMC by minimizing errors and standard deviations as much as possible.

In this regard, if it is possible to directly measure the desired value, various studies have been carried out on algorithms for selecting sequential observation locations that are expected to maximize the accuracy based on the estimation results of the corresponding values using the previous observations results (Kleijnen *et al.*, 2011; Matthias, 1997; Picheny *et al.*, 2010). However, since the algorithms and methodologies proposed in these researches assume that the desired value can be observed directly, it is difficult to use these algorithms and methodologies directly for system identification.

This study proposes a method for selecting the direct sequentially observed location, which is expected to maximize the system identification accuracy of the indirectly estimated value by using the results of the aforementioned researches.

1.2. Research Objectives

The goal of this study is to indirectly estimate the effective thickness of a structure with the highest accuracy under a small number of strain observations. From the contents described in Chapter 1.1, the indirectly estimated value is selected as the effective thickness of the structure, and the directly measured value is selected as a strain of the structure.

When selecting the strain measurement location for system identification, observation locations for increased accuracy are changed depending on the state of the load acting on the structure and the actual effective thickness distribution of the structure. Therefore, it would be more effective to sequentially select the observation locations that are supposed to maximize the accuracy by using the applied load and the estimated effective thickness distribution, rather than intuitive selection of observation locations simultaneously. Consequently, this study uses the sequential optimization method to select the next strain measurement location where the highest accuracy improvement is expected based on the estimated effective thickness distribution.

The optimization technique used in this study is divided into two steps. The first step is to measure the strain at the previously determined location, and then to estimate distribution of the effective thickness using the measured values. Here, the previously determined location is arbitrary initial locations at the beginning, and the selected next strain measurement locations are added afterwards.

The second step is to determine the next strain measurement location using the

estimated effective thickness. The strain measurement location is chosen to satisfy two goals: minimize the error between the estimated effective thickness and the actual effective thickness; and minimize the standard deviation of the estimated effective thickness. The two steps are iterated to finally determine the effective thickness under a limited number of strain measurements. Figure 1.2 briefly summarizes the optimization process of this study.

This study is divided into three parts. In the first part, the effective thickness distribution of the structure is estimated using the directly observed strain values. In the second part, three methods are proposed to select the next strain measurement location using the estimation result. In the third part, the proposed methodology is verified as a numerical example using a plate structure. Comparing the results of each phase between the proposed methodologies, and also comparing the final results of the proposed methodology with intuitively and simultaneously selected observation positions.

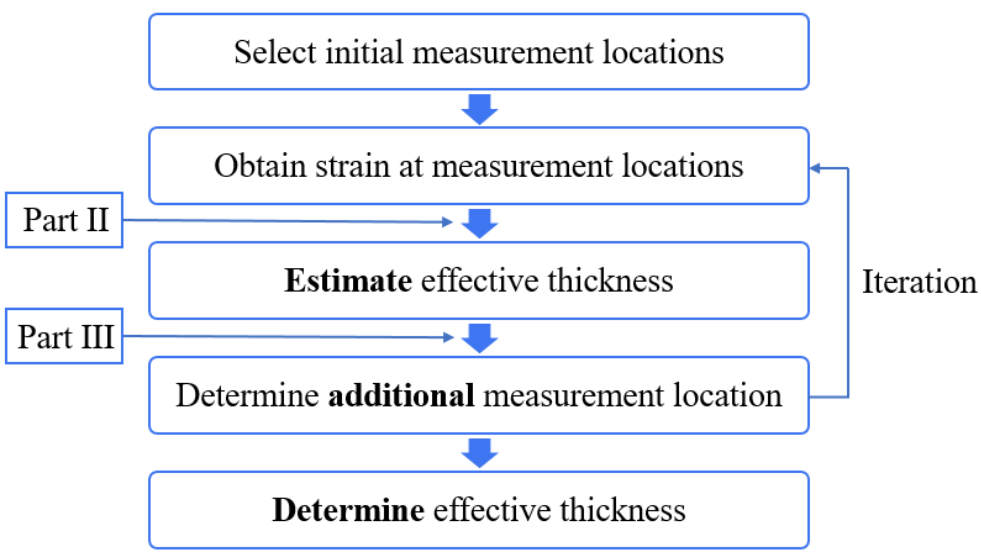

Figure 1.2. Summary of the optimization process in this study

1.3. Outline

Chapter 1 proposes the research background, research objectives, and outline of this study.

Chapter 2 estimates the average and standard deviation of the effective thickness at each node of the structure. For this goal, this chapter first presents theoretical explanations of Karhunen-Loève expansion, Bayesian updating and MCMC.

Chapter 3 proposes three methods for generating effective thickness samples of a structure using the average and standard deviation of the estimated effective thickness in Chapter 2. First, explain each sample generation method and compare the strengths and the weaknesses. Next, describe how to select the next strain observation position using the generated sample effected thickness, and define the value named ‘Sensitivity of Strain Variation’ for this purpose.

Chapter 4 verifies the proposed methodology using numerical examples with steel plate structures. The numerical examples are divided into three types according to the direction of the strain. Each example first compares the results of each of the phases between the proposed methodologies. The validity of the proposed methodology is then verified by comparing the final results of the proposed methodology with intuitive and simultaneous selection of observation locations.

Chapter 5 summarizes the study and provides academic and practical implications, study limitations, and suggestions for future research.

Chapter 2. System Identification of Structures by Physical Measurements

The first step of indirect measurement locations optimization for accurate system identification of structures is to estimate the distribution of the material properties by using the measured observations at the specified measurement location. For this goal, this chapter first introduces Karhunen-Loève Expansion which can approximate an arbitrary distribution of material properties with a combination of specific random variables. Next, the process is explained that how to obtain the information of the random variables of the Karhunen-Loève Expansion through Bayesian updating using MCMC from the measured observations. Finally, a method is proposed to estimating the distribution of indirectly estimated material properties of structures.

2.1. Karhunen-Loève Expansion

Kari karhunen and Michel Loève proved that an arbitrary stochastic process is represented by a linear combination of infinite orthogonal functions, and this is called the Karhunen-Loève Theorem (Karhunen, 1947; Loeve, 1963). In addition, the linear combination of functions in this theorem is called the Karhunen-Loève expansion (K-L expansion). K-L expansion accurately preserves the stochastic properties of the stochastic process, such as the average and auto-covariance.

The stochastic process in this study is restricted to the two-dimensional Gaussian random field used to represent the uncertain deterioration state of the structure in Yi and Song (2018). K-L expansion formularizes an arbitrary random field $w(x, y)$ as follows:

$$w(x, y) = \overline{w} + \sum_{i=1}^{\infty} \sqrt{\lambda_i} \varphi_i(x, y) \xi_i \tag{2.1}$$

where $\overline{w}$ is the mean of the random field, and $\xi_1,\ \xi_2, \ldots$ are independent standard normal random variables to determine the distribution shape of the random field. $\xi_1,\ \xi_2, \ldots$ are generally called KL random variables, and these are used as weights of λ_i and φ_i. λ_i and φ_i are deterministic values that determine the correlation property. λ_i and φ_i can be obtained by solving the Fredholm integral equation of the second kind:

$$\int_D C(x_1, x_2) \varphi_i(x_2) dx_2 = \lambda_i \varphi_i(x_1) \tag{2.2}$$

where $C(x_1, x_2)$ is the autocovariance function of the random field $w(x, y)$, λ_i is the eigenvalue, and φ_i is the orthogonal eigenfunction which is a solution of Equation (2.2). Various numerical solutions depending on the type of basis eigenfunction to obtaining λ_i and φ_i have been studied (Betz *et al.*, 2014; Ghanem & Spanos, 1991). In this study, λ_i and φ_i are obtained using the finite element method using piecewise polynomial basis.

Ignoring the case when the λ_i is small, the following truncated K-L expansion can be obtained.

$$w(x,y) \cong \widehat{w}(x,y) = \overline{w} + \sum_{i=1}^{k} \sqrt{\lambda_i}\varphi_i(x,y)\xi_i \quad (2.3)$$

This truncated K-L expansion also shows sufficiently small errors when using a small number of KL random variables (Huang *et al.*, 2001). Therefore, it is assumed that the effective thickness distribution of the structure can be approximately formularized by using a small number of KL random variables.

2.2. Obtain Samples of KL Random Variables by Bayesian Inference and Markov Chain Monte Carlo

Suppose the autocovariance function of the effective thickness of a given structure is already known. Then, the effective thickness distribution of the structure can be obtained by determining the mean of the effective thickness and the KL random variable in Equation (2.3). To determine the values of these random variables, this study uses the Bayes' rule with evidence of previously observed strain values at specific locations in the structure. If the previously observed strain values are given as $\boldsymbol{\varepsilon}^m = \{\varepsilon_n^m\}, n = 1, \dots, N$, the posterior probability is obtained as follows (Yi & Song, 2018):

$$P(\xi_1, \xi_2, \dots, \xi_k, \overline{w} | \boldsymbol{\varepsilon}^m) = c \cdot L(\boldsymbol{\varepsilon}^m | \xi_1, \xi_2, \dots, \xi_k, \overline{w}) \cdot P(\xi_1, \xi_2, \dots, \xi_k, \overline{w}) \quad (2.4)$$

where c is a normalizing constant, and $L(\boldsymbol{\varepsilon}^m | \xi_1, \xi_2, \dots, \xi_k, \overline{w})$ is the likelihood function. Independent standard normal distribution is used as the prior distribution

of KL random variables. In addition, previously observed strain values are not related to the direction of strain, but using z-direction strain is avoided because observe z-direction strain is relatively difficult.

Suppose the effective thickness distribution determined by any given random variables $\xi_1, \xi_2, \ \ldots, \xi_k, \overline{w}$. Assume that ε_n^r is the strain value at the location where the strain value is ε_n^m, and strain measurement data follow an independent normal distribution with variance σ_n^2. Therefore, likelihood $L(\boldsymbol{\varepsilon}^m|\xi_1, \xi_2, \ \ldots, \xi_k, \overline{w})$ can be obtained as follows:

$$\begin{aligned} L(\boldsymbol{\varepsilon}^m|\xi_1, \xi_2, \ \ldots, \xi_k, \overline{w}) &= \prod_{n=1}^{N} L(\varepsilon_n^m|\xi_1, \xi_2, \ \ldots, \xi_k, \overline{w}) \\ &= \prod_{n=1}^{N} P(\varepsilon_n^r = \varepsilon_n^m) = \prod_{n=1}^{N} \phi\left(\frac{\varepsilon_n^r - \varepsilon_n^m}{\sigma_n}\right) \end{aligned} \tag{2.5}$$

where ϕ is the probability density function of the standard normal distribution.

If it is possible to find $\xi_1, \xi_2, \ \ldots, \xi_k, \overline{w}$ with the largest $P(\xi_1, \xi_2, \ \ldots, \xi_k, \overline{w}|\boldsymbol{\varepsilon}^m)$ for given $\boldsymbol{\varepsilon}^m$ in the Equation (2.4), the effective thickness distribution of the structure can be estimated by substitute these random variables to the K-L expansion. Normalization constant c is formularized by Equation (2.6). However, there is a serious problem: the larger the number of KL random variables, the more exponentially the computational cost. Therefore, it is almost impossible to directly compute the integral:

$$c = \int \ldots \int L(\varepsilon^m|\xi_1, \xi_2, \ \ldots, \xi_k, \overline{w}) P(\xi_1, \xi_2, \ \ldots, \xi_k, \overline{w}) \, d(\xi_1, \xi_2, \ \ldots, \xi_k, \overline{w}) \tag{2.6}$$

To overcome this difficulty, a study of Bayesian updating using Markov chain Monte Carlo(MCMC) sampling method was performed (Yi & Song, 2018). Instead of calculating the normalization constant c directly, Yi and Song (2018) select the next random variable samples using the current random variables and independent posterior distribution and compare the probability of two random variable sample sets under a given strain observation through the likelihood and prior distribution to determine whether to choose a new sample. The Metropolis-Hastings algorithm was used to generate the Markov chain. Repeating the above steps, therefore the Markov chain $\left\{\xi_i^{(1)}, \xi_i^{(2)}, \dots, \xi_i^{(N_{MC})}\right\}, \left\{\overline{w}^{(1)}, \overline{w}^{(2)}, \dots, \overline{w}^{(N_{MC})}\right\}$ is generated directly for each random variable without calculating normalization constant c, where N_{MC} is the length of the Markov chain. Finally, the distribution of each random variable can be estimated using the generated Markov chain. In this regard, some number of samples at the beginning until the Markov chain reaches the stationary distribution are ignored as a burn-in period (Dickinson *et al.*, 1993).

2.3. Estimate Distribution of the Effective Thickness

Mean and standard deviation of the effective thickness can be estimated under given strain observations by the contents of Chapter 2.1 and 2.2. This is largely divided into three steps.

The First step is to estimate the mean of the effective thickness $\overline{w}$ using the Bayesian updating method. Before obtaining the KL random variables $\{\xi_i\}$, it is desirable to obtain the mean of the effective thickness because the initial value

setting is very important for Bayesian updating of other KL random variables. It is serious problem that the probability decreases very rapidly as the difference between the predicted value and the actual value increases. If the difference between the predicted initial value and the actual value is large, the prior distribution probability of $\overline{w}$ becomes extremely small that it cannot be calculated exactly, and this makes a serious problem in comparing the prior and posterior probabilities of KL random variables. Therefore, to avoid the situation where the KL random variables generate a meaningless Markov chain, $\overline{w}$ that has the highest probability of mean of random field is estimated by Bayesian updating before the Markov chain generation of KL random variables. Since the value of KL random variables are not known when $\overline{w}$ is pre-estimated, assume that $\{\xi_i\} = 0,\ i = 1, \dots, k$ considering that KL random variables follow an independent standard normal distribution. The first step produces a single Markov chain for $\overline{w}$, therefore it needs a relatively short Markov chain, and sets the length of the burn-in period short either. An example of the generated Markov chain of $\overline{w}$ is shown in Figure 2.1.

From the Markov chain, it is possible to obtain $\hat{\overline{w}}_{temp}$ which is the expected value of $\overline{w}$ as follows:

$$\hat{\overline{w}}_{temp} = \frac{1}{N_1 - b_1} \sum_{j=b_1}^{N_1} \overline{w}_{temp}^{(j)} \tag{2.7}$$

where N_1 is the total length of the first step's Markov chain, b_1 is the length of the burn-in period of the first step's Markov chain, and $\overline{w}_{temp}^{(j)}$ is the jth Markov chain value of $\overline{w}$ under the assumption of $\{\xi_i\} = 0,\ i = 1, \dots, k$.

The second step is to estimate the KL random variables $\{\xi_i\}$ using the same Bayesian updating method as in the first step. Estimating the KL random variables requires a much longer Markov chain than estimating $\bar{w}$, because the larger the number of KL random variables, the longer the Markov chain length until the chain reaches the stationary distribution. Moreover, it is also the reason for the increase of the length of the Markov chain which the standard deviation of each ξ_i is much larger than the standard deviation of $\bar{w}$. The length of the burn-in period is also relatively long compared to the first step. In addition, the Markov chain of $\bar{w}$ must be obtained again because the $\widehat{\bar{w}}_{temp}$ value obtained in the first step is a value obtained by assuming $\{\xi_i\} = 0,\ i = 1, \dots, k$ temporarily for setting the initial value of $\bar{w}$ in the second step. An example of the generated Markov chain of $\{\xi_i\}$ and $\bar{w}$ is shown in Figure 2.2.

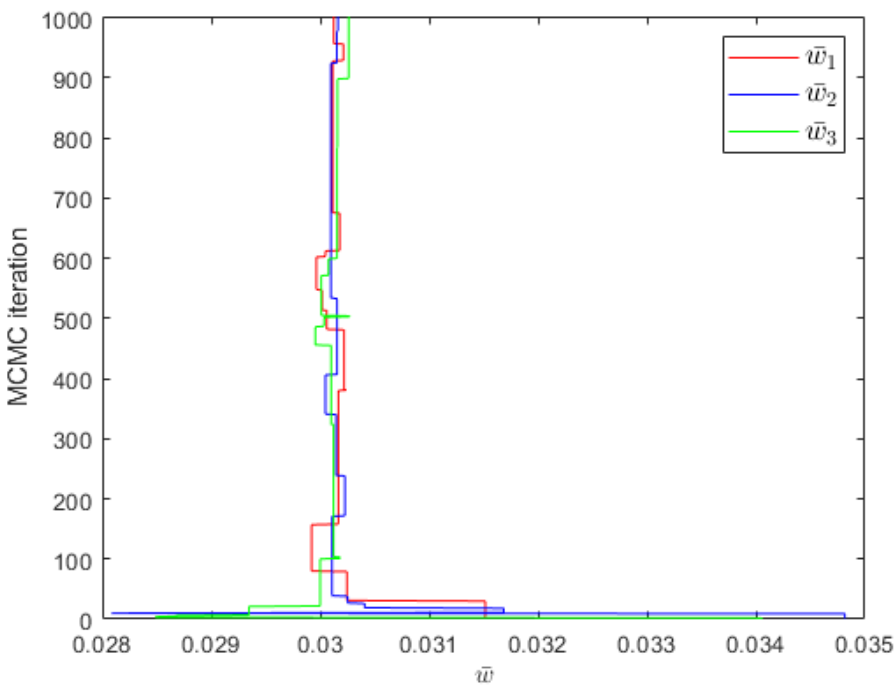

Figure 2.1. Three different Markov chains of $\bar{w}$

From the Markov chain of the random variables of K-L expansion, it is possible to determine the expected values $\{\hat{\xi}_i\}$ and $\hat{\bar{w}}$ as follows:

$$\hat{\xi}_i = \frac{1}{N_2 - b_2} \sum_{j=b_2}^{N_2} \xi_i{}^{(j)} \quad (i = 1, \dots, k) \tag{2.8a}$$

$$\hat{\bar{w}} = \frac{1}{N_2 - b_2} \sum_{j=b_2}^{N_2} \bar{w}^{(j)} \tag{2.8b}$$

where N_2 is the total length of the second step's Markov chain, b_2 is the length of the burn-in period of the second step's Markov chain, and $\xi_i{}^{(j)}$ and $\bar{w}^{(j)}$ are the jth Markov chain values of ξ_i and $\bar{w}$.

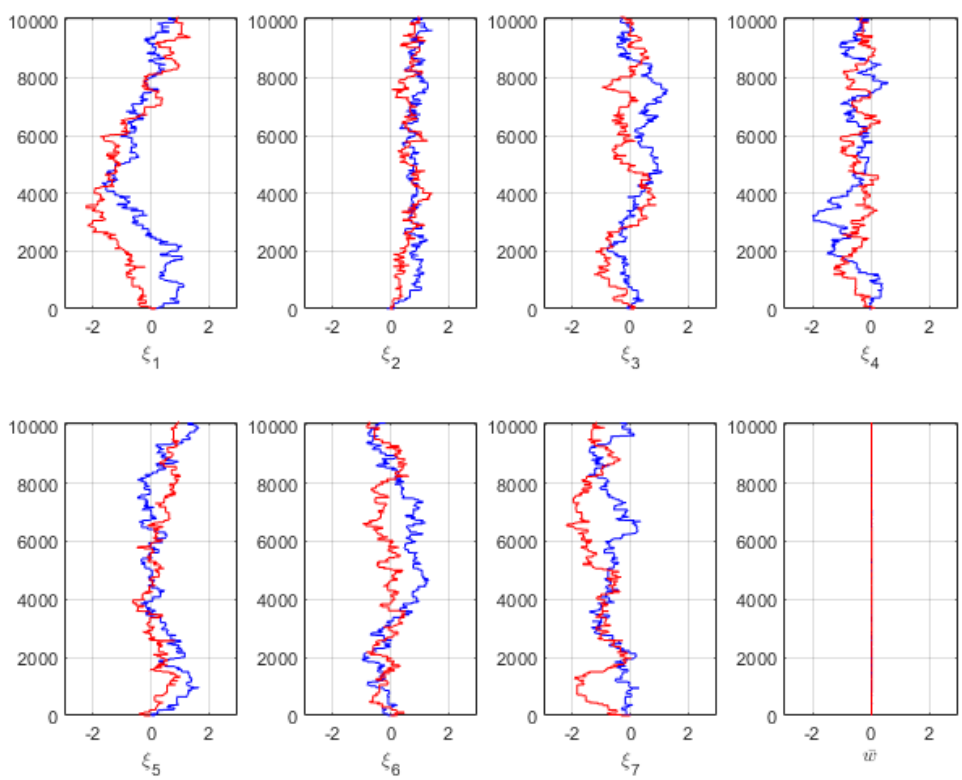

Figure 2.2. Two different Markov chains of $\{\xi_i\}$ and $\bar{w}$

The final step is to estimate the mean and standard deviation of the effective thickness at each node by using the Markov chain of each random variable obtained in the second step. First, the Markov chain of w for each node is obtained by substituting the Markov chain of ξ_i and $\overline{w}$ into Equation (2.3). Next, use the following equation to obtain the expected mean of the effective thickness at each node:

$$\widehat{w} = \frac{1}{N_2 - b_2} \sum_{j=b_2}^{N_2} w^{(j)} \tag{2.9}$$

Equation (2.9) have the same form of Equations (2.8a) and (2.8b) that obtain $\{\widehat{\xi_i}\}$ and $\widehat{\overline{w}}$ which are expected values of $\{\xi_i\}$ and $\overline{w}$. Alternatively, the same result can be obtained by substituting $\{\widehat{\xi_i}\}$ and $\widehat{\overline{w}}$ obtained from Equations (2.8a) and (2.8b) into Equation (2.3), since w in the K-L expansion is a linear combination of ξ_i and $\overline{w}$. At last, calculate $\hat{\sigma}_w$ which is the expected value of the standard deviation of the effective thickness at each node. $\hat{\sigma}_w$ can be obtained as follows using the Markov chain of w $\{w^{(1)}, w^{(2)}, \dots, w^{(N_2)}\}$ for each node obtained above:

$$\hat{\sigma}_w^2 = \frac{\tau_w}{N} Var\left[\{w^{(j)}\}\right] \tag{2.10}$$

where τ_w is the integration autocorrelation time of w defined as Equation (2.11a), (2.11b), and (2.11c) (Goodman & Weare, 2010):

$$\tau_w = \hat{\tau}_w(M_t) = 1 + 2 \sum_{\tau=1}^{M_t} \hat{\rho}_w(\tau) \tag{2.11a}$$

$$\hat{\rho}_w(\tau) = \frac{\hat{c}_w(\tau)}{\hat{c}_w(0)} \tag{2.11b}$$

$$\hat{c}_w(\tau) = \frac{1}{N_2 - \tau} \sum_{j=1}^{N_2-\tau} \left(w^{(j)} - \frac{1}{N_2} \sum_{k=1}^{N_2} w^{(k)} \right) \left(w^{(j+\tau)} - \frac{1}{N_2} \sum_{k=1}^{N_2} w^{(k)} \right) \tag{2.11c}$$

where M_t is the minimum value of M which satisfies $M - \hat{\tau}_w(M) > 0$, and $\hat{\rho}_w(\tau)$ is called normalized autocorrelation function.

Using the mean and standard deviation of the effective thickness obtained by Equation (2.9) and (2.10), the confidence interval of the effective thickness over the structure can be estimated as shown in Figure 2.3.

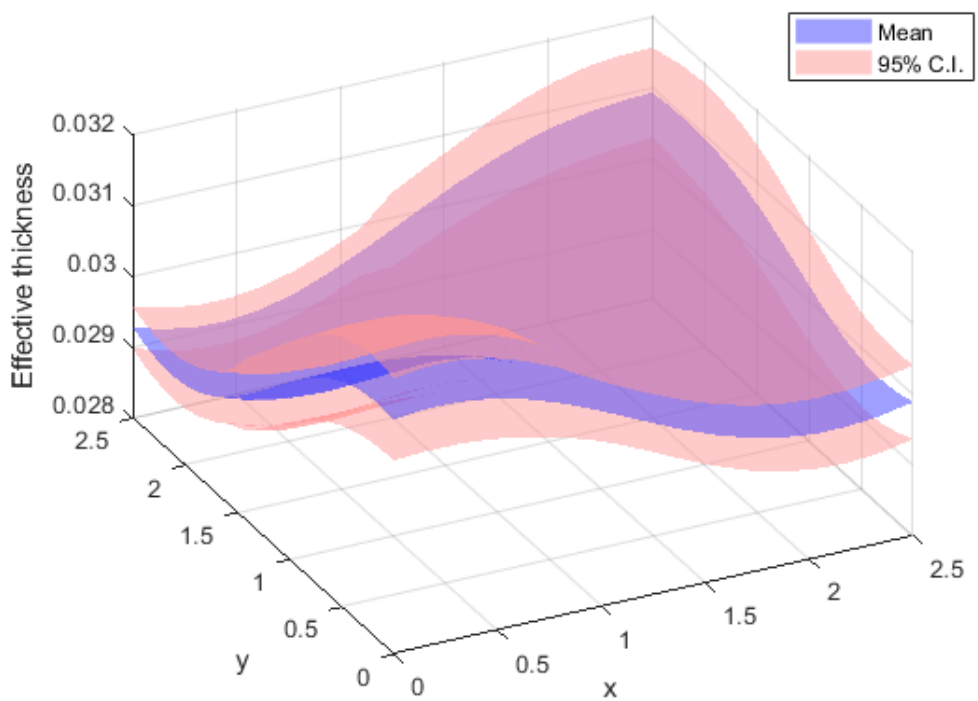

Figure 2.3. Mean(blue) and 95% confidence interval(red) of the effective thickness

Chapter 3. Sequential Selection Technique of Measurement Locations

The second step of indirect measurement locations optimization for accurate system identification of structures is to select the next directly measurement location which can increase the accuracy of indirect estimation as much as possible. This study proposes and compares three sequential measurement location selection methods.

3.1. Goal of Measurement Locations Selection

The goal of this study is to maximize the accuracy of the effective thickness estimation as much as possible. Increasing the accuracy of the effective thickness estimation can be roughly divided into two goals. The first is to minimize the error between the estimated mean of the effective thickness and the actual effective thickness. The reliability of the average of the estimated effective thickness lowered when the estimated mean of the effective thickness is significantly different from the actual effective thickness. Therefore, when using the same number of observed data, it is necessary to select the observation location where the error is minimized. The other is to reduce the standard deviation of the predicted effective thickness as much as possible. If the standard deviation of the predicted effective thickness is large, the probability that the difference between the estimated mean of the effective thickness

and the actual effective thickness becomes large. Consequently, the range of the confidence interval of the effective thickness becomes wider. This should be avoided because it may cause excessive conservative judgement when determining the stability of buildings.

If it is possible to measure the effective thickness directly, the effective thickness on the structure can be estimated directly by apply Kriging (Ginsbourger *et al.*, 2010) or Gaussian Process (Rasmussen & Williams, 2006) to the measured effective thickness data. In addition, sequential direct measurement location selection of the effective thickness is also possible using Efficient Global Optimization(EGO) algorithm and Expected Improvement (Jones *et al.*, 1998). However, the effective thickness is not directly measurable value. Therefore, by using the directly observed strain data and the effective thickness distribution of the structure obtained by observed strain, it is desirable to determine the next strain measurement location which is expected to maximize the accuracy of the estimated effective thickness. However, since the relationship between the effective thickness and the strain is complex nonlinear, it is practically impossible to analytically represent the next strain measurement location using the estimated effective thickness distribution. Instead of analytical method, the experimental method is used.

In order to select the strain measurement location that is expected to maximize the accuracy of the effective thickness estimation, the following procedure is performed: First, artificially generate various effective thickness distribution samples using the results obtained in Chapter 2. Next, obtain distributions of the strain when the loads are applied to the structures having each sample effective thickness. Finite element method is used to obtain the distributions of the strain.

Finally, find the location where the strain varied largest when the distribution of the effective thickness changes. The corresponding location is selected as the most sensitive location of the strain, and also used as the next strain measurement location. In Chapter 3.2, this study proposes various methods to generate effective thickness distribution samples. In Chapter 3.3, this study proposes a method to select the most sensitive location, i.e. the next strain measurement location, using the sample effective thickness distribution.

3.2. Methods to Generate Sample Effective Thickness

This chapter proposes three different methods of generating the effective thickness distribution sample, and compares the advantages and disadvantages of each method.

3.2.1. Scheme 1: Sampling specific effective thickness

The first scheme is to generate effective thickness distribution samples considering only the standard deviation of the specific location where the standard deviation of the effective thickness is greatest. This scheme requires one assumption before starting: the estimated effective thickness at the location where the strain measured is the exact value. In this case, the above assumption is made because the effective thickness at the location where the strain is measured has a high probability of being accurate.

First, find the node with the largest standard deviation of the effective thickness

throughout the entire structure. Then, sampling the effective thickness at the corresponding node. Assume that the distribution of the effective thickness at the node follows the Gaussian distribution with the mean $\hat{w}$ and variance $\hat{\sigma}_w^2$ obtained in Chapter 2.3. Next, perform a Gaussian process using the sampled effective thickness and the estimated effective thickness at the strain measurement location. For the implementation of the Gaussian process, accurate effective thickness at some locations are needed. This is the reason why the effective thickness estimation at the strain measurement location is assumed to be an accurate value. Finally, the results of the Gaussian process are used as the effective thickness distribution sample of the entire structure. Figure 3.1 shows the example of the entire standard deviation of the estimated effective thickness, the location where the standard deviation of the effective thickness is maximum, and the location where the strain is already measured. Using the results from Figure 3.1, examples of effective thickness distribution samples obtained from Scheme 1 can be seen in Figure 3.2.

Because Scheme 1 changes only the effective thickness of one node, the number of the situation is very limited. Therefore, a very small number of samples can confirm various cases, and this means that the calculation cost of Scheme 1 is very low. However, since the standard deviation at other nodes excepting the node with the largest standard deviation is considered only by the result of the Gaussian process, it can be applied differently from the actual standard deviation. Therefore, locations of sequential strain observation using Scheme 1 have a relatively lower effect. Furthermore, an additional problem is that the estimated effective thickness at the strain measured location is not actually an exact value, i.e. there exist standard deviation of the effective thickness at the strain measurement location.

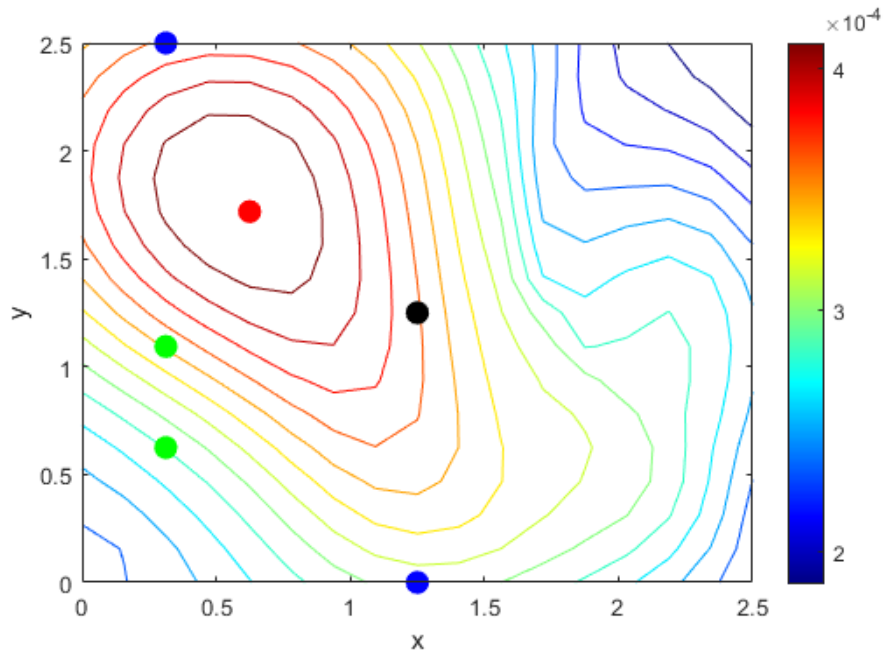

Figure 3.1. Distribution of the estimated effective thickness standard deviation

Red: Maximum standard deviation, Others: Strain measurement locations

Blue: x direction, Green: y direction, Black: both direction

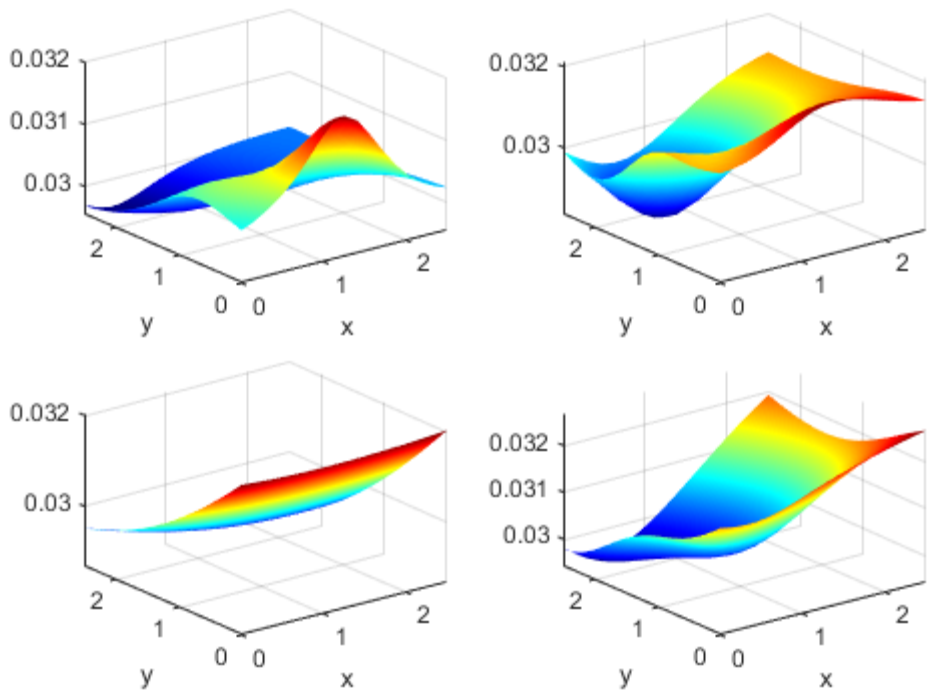

Figure 3.2. Examples of effective thickness samples obtained from scheme 1

3.2.2. Scheme 2: Sampling whole effective thickness

The second scheme is to directly consider the standard deviation of the effective thickness at all nodes. This scheme independently sampling the effective thickness at all nodes of the structure. Similar to the Scheme 1, Scheme 2 assumed that the distribution of the effective thickness at each node follows the independent Gaussian distribution with the mean $\hat{w}$ and variance $\hat{\sigma}_w^2$ at each node obtained in Chapter 2.3. Effective thickness independently sampled at each node are directly used as the effective thickness distribution sample of the structure. Figure 3.3 shows an example of the effective thickness distribution sample obtained through the Scheme 2 procedure.

Scheme 2 generates effective thickness samples that directly consider the standard deviation of the effective thickness at all nodes. Therefore, the location of sequential strain observation using Scheme 2 will have a relatively higher effect. However, since Scheme 2 independently samples the effective thickness at all nodes, the diversity of situations in Scheme 1 exists independently at all nodes of Scheme 2. This implies that Scheme 2 requires a large number of samples in exponential order compared to Scheme 1 in order to sufficiently confirm the number of cases, and this requires a very high computational cost. In addition, since the effective thickness at each node is sampled independently, there is a problem in that correlation of effective thicknesses of adjacent nodes cannot be considered. This means that the sample effective thickness distribution obtained from Scheme 2 is unrealistic when compared to samples obtained from other schemes.

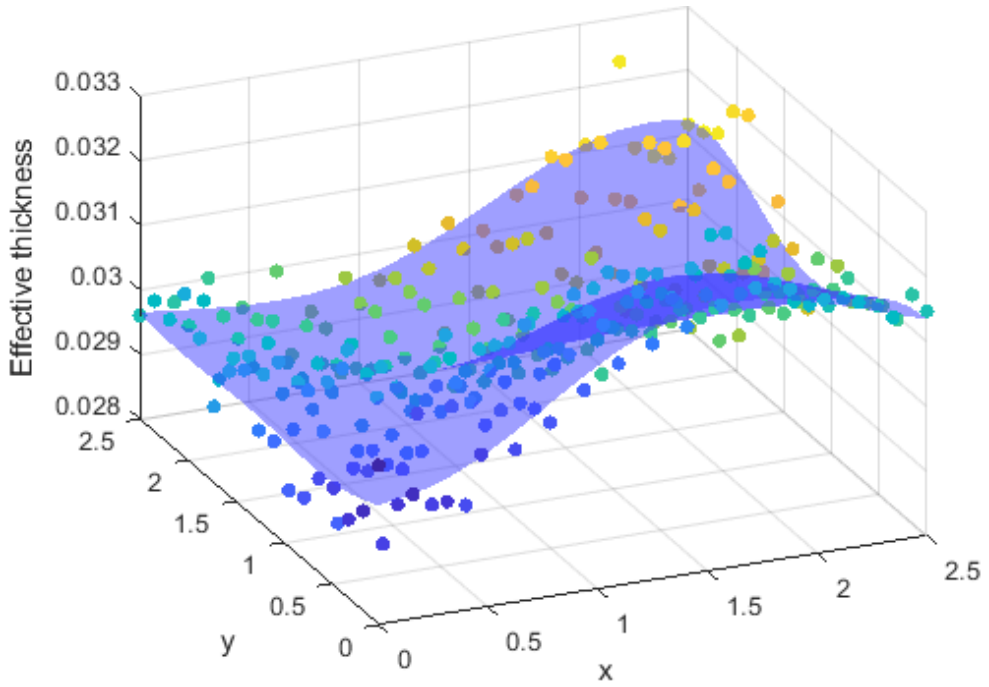

Figure 3.3. Example of effective thickness samples obtained from Scheme 2

3.2.3. Scheme 3: Sampling random variables of K-L expansion

The third scheme is to indirectly consider the standard deviation of the effective thickness at all nodes. Scheme 1 and Scheme 2 directly sampled the effective thickness at the nodes, but Scheme 3 sampling the random variables in the K-L expansion equation instead of the effective thickness at the nodes.

First, samples a value for each random variable $\{\xi_i\}$ and $\overline{w}$ in the Markov chain obtained in Chapter 2.3. Note that the burn-in period should be excluded from the range of sample. Next, substitute sampled random variables to Equation (2.3). The result of the substitution is used as the sample of the effective thickness distribution of the structure. Figure 3.4 shows an example of sampling the value of each random variable in the Markov chain, and Figure 3.5 shows the process of

obtaining the sample of the effective thickness distribution through the Scheme 3 procedure using the results of Figure 3.4.

Scheme 3 samples KL random variables $\{\xi_i\}$ and the mean of the effective thickness $\overline{w}$. Among them, KL random variables $\{\xi_i\}$ are used as the weight of the orthogonal eigenfunction φ_i of Equation (2.2).

$$\int_D C(x_1, x_2)\varphi_i(x_2)dx_2 = \lambda_i\varphi_i(x_1) \tag{2.9}$$

Since the orthogonal eigenfunction is a function having a predetermined value depending on the structure, an estimated effective thickness of the entire structure is also changed when the values of KL random variables are changed. Finally, Scheme 3 also generates a sample of effective thickness that is indirect but considers the standard deviation of effective thickness at all nodes. Therefore, the location of sequential strain observation using Scheme 3 will also have a relatively higher effect, similar to the Scheme 2. Moreover, Scheme 3 only requires sampling of the random variables of K-L expansion, and the number of random variables is $k + 1$ based on Equation (2.3).

Therefore, Scheme 3 has relatively larger number of possible cases than Scheme 1, but it has exponentially smaller number of possible cases than Scheme 2. This means that the number of required samples is relatively small, and it means that the required computational cost is low. However, if the number of strain observations is less than the number of random variables, it is difficult to clearly determine whether some random variables reach the stationary distribution. This makes an additional problem that the difference depending on the length of the burn-in period is large.

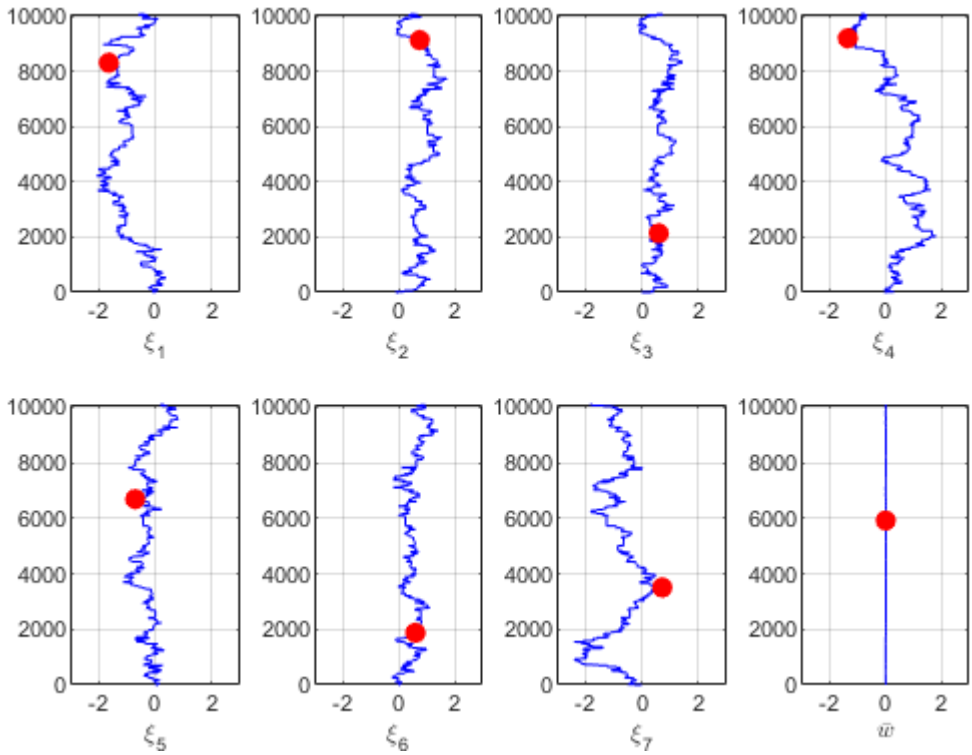

Figure 3.4. Example of sampling each random variable in the Markov chain

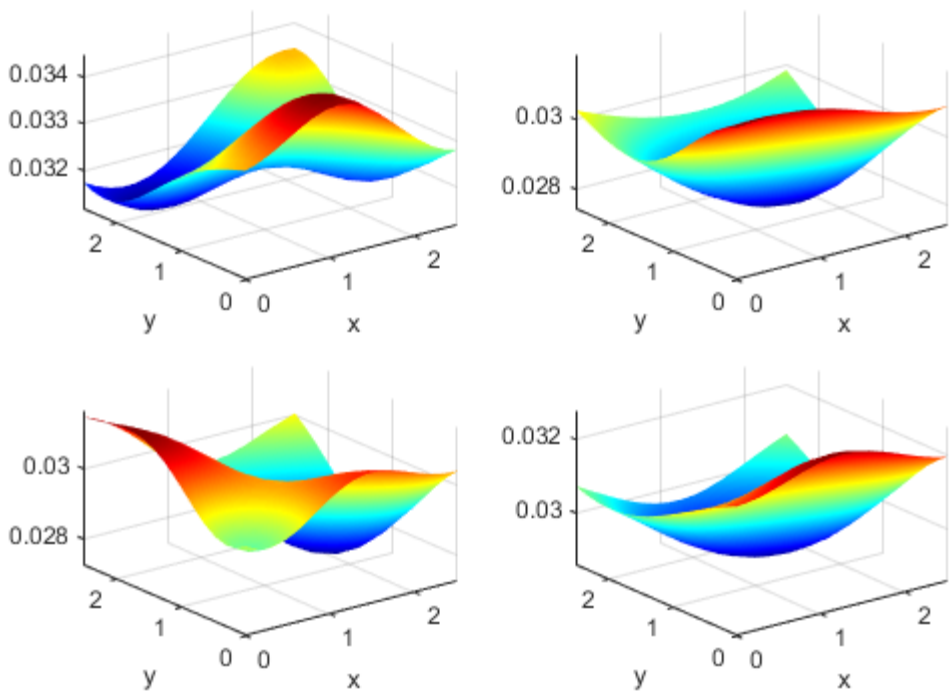

Figure 3.5. Examples of effective thickness samples obtained from Scheme 3

3.2.4. Comparison between sample effective thickness generation methods

Schemes 1~3 presented above are summarized in Table 3.1. From the viewpoint of required calculation cost, Scheme 2 is the most expensive, and Scheme 1 is the least expensive. From the viewpoint of expected effects, Scheme 2 and Scheme 3 are expected to be the most accurate, and Scheme 1 is expected to be the least accurate.

	Scheme 1	**Scheme 2**	**Scheme 3**
Sampling variables	Effective thickness of node which has maximum standard deviation	Effective thickness of all nodes	Random variables of K-L expansion ($\{\xi_i\}$ and $\overline{w}$)
Number of sampling variables	1 node	Number of nodes	Number of random variables of K-L expansion
Required calculation cost	Very Low	High	Low
Expected effects	Low	High	High
Other weakness	Estimated effective thickness at the location where the strain is measured is not an exact value	Correlation of effective thicknesses of adjacent nodes cannot be considered	Difference depending on the length setting of the burn-in period is large

Table 3.1. Comparison between methods to generate sample effective thickness

3.3. Methods to Determine Additional Measurement Location Using Samples

The final process of this method is to select the sequential strain measurement locations using the sample of the effective thickness distribution which obtained previously. Using the finite element method, it is possible to obtain the strain at each node for each effective thickness sample by applying loads to the effective thickness sample of the structure. Since the strain value is measurable, it can be deduced that the standard deviation of the effective thickness can be reduced as much as possible by measuring the strain at the location where the strain is the most uncertain, i.e. where the change of strain is largest. Therefore, it is concluded that the location where the strain changes most is the most sensitive location when the effective thickness distribution is changed.

However, selecting the next strain measurement location as the largest change of the strain amount causes a serious problem. The reason is that the location where the strain changes most when the distribution of the effective thickness changes is near the location where the absolute value of the strain is largest.

For a simple example, consider the case where the equally distributed load acts on the entire simply supported beam with uniform effective thickness as shown in Figure 3.6. The deflection of the beam by the load is the solid line in Figure 3.7. If the effective thickness of the simply supported beam is uniformly reduced, the shape of the loaded beam changes to the dotted line in Figure 3.7. In other words, the strain is equally zero at the supported locations, and as the distance from the supported

location increases, the amount of strain variation increases. Finally, the amount of strain variation at the center of the beam is the maximum.

This is similar to the case where the effective thickness of the part of the beam is reduced instead of the entire beam. For example, consider the case when the effective thickness decreases only in the right half of the beam. In this case, when the load is applied, the shape of the loaded beam changes to the dashed line in Figure 3.7. Since the increase of strain is slow in the left half of the beam where the effective thickness is thick, and the increase of strain is fast in the right half of the beam where the effective thickness is thin. As a result, the location with the maximum strain is shifted to the right. However, since the change of the effective thickness is generally very small, the maximum strain location in this situation is almost the same as the center of the beam having the maximum strain before. Therefore, the location at which the amount of strain increase is maximum is also generated at a similar location.

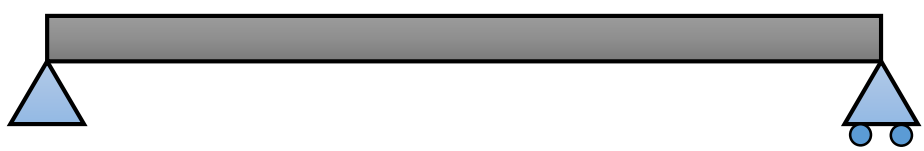

Figure 3.6. Simply supported beam

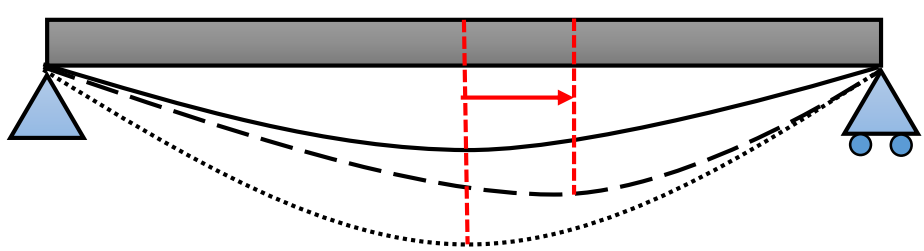

Figure 3.7. Deformation of simply supported beam in three effective thickness distributions

For these reasons, it is difficult to use the raw observed strain data for the decision of the next measurement location. Alternatively, considering the fact that the amount of change of the strain and the absolute value of the strain is proportional. Therefore, the ratio of the amount of change of the strain to the absolute value of the strain could be used for determining the strain measurement location. However, it is difficult to determine the next strain measurement location by the ratio of the amount of change of the strain either, because the ratio can diverge to infinity at the location where the absolute value of the strain is close to zero.

This study will determine the location of the next strain measurement by using the deviation of the strain of the node that makes up each element used in the finite element analysis of the structure. It is difficult to use the strain value raw data at each node because of the reason explained above. Therefore, this study considers elements instead of nodes. Calculate the difference of the maximum strain value and the minimum strain value of the nodes constituting each element, and check how much the difference varies with the change of the effective thickness. The difference of the maximum and minimum values of the strain in each element means the degree of deformation of the element. Here, a large change in the difference of the strain in the element means that the deformation of the element changes greatly. Therefore, there is a direct correlation between selecting the location with the greatest strain variation.

In order to determine the location of the next strain measurement using the strain deviation of the element, a value named ‘Sensitivity of Strain Variation’(SSV) is defined. This value determines whether the strain variation is sensitive to the effective thickness variation, and is defined as follows:

$$\text{SSV of the element} = \frac{1}{n}\sum_{i=1}^{n}\frac{\max\left(\varepsilon_{max}^{m} - \varepsilon_{min}^{m},\ \varepsilon_{max}^{s_i} - \varepsilon_{min}^{s_i}\right)}{\min\left(\varepsilon_{max}^{m} - \varepsilon_{min}^{m},\ \varepsilon_{max}^{s_i} - \varepsilon_{min}^{s_i}\right)} \quad (3.1)$$

where each value is defined as follows, and the subscript of strain refers to the vertex nodes in the square elements used in the finite element analysis of this study, shown in Figure 3.8.

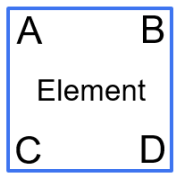

Figure 3.8. Square element

- ε^{m}: strain when the effective thickness is mean value
- ε^{s_i}: strain when the effective thickness is *i*-th sample (the number of total sample = n)
- $\varepsilon_{max}^{m} = \max(\varepsilon_{A}^{m},\ \varepsilon_{B}^{m},\ \varepsilon_{C}^{m},\ \varepsilon_{D}^{m})$
- $\varepsilon_{min}^{m} = \min(\varepsilon_{A}^{m},\ \varepsilon_{B}^{m},\ \varepsilon_{C}^{m},\ \varepsilon_{D}^{m})$
- $\varepsilon_{max}^{s_i} = \max\left(\varepsilon_{A}^{s_i},\ \varepsilon_{B}^{s_i},\ \varepsilon_{C}^{s_i},\ \varepsilon_{D}^{s_i}\right)$
- $\varepsilon_{min}^{s_i} = \min\left(\varepsilon_{A}^{s_i},\ \varepsilon_{B}^{s_i},\ \varepsilon_{C}^{s_i},\ \varepsilon_{D}^{s_i}\right)$

In the SSV value, $\varepsilon_{max}^{m} - \varepsilon_{min}^{m}$ is the difference between the maximum and minimum values of the strain within the square element when the effective thickness is mean, and $\varepsilon_{max}^{s_i} - \varepsilon_{min}^{s_i}$ is the difference between the maximum and minimum values of the strain within the square element when the effective thickness is *i*-th sample. In conclusion, in the definition of SSV, the equation inside the summation is a value indicating how much the strain of the element changes in each sample

effective thickness distribution. This is consistent with the goal of obtaining the variance of the elements.

The basic method for determining the next strain measurement location using the SSV value is to set the next strain measurement location where the SSV value is maximum. However, since the SSV value defined above is determined for each element, the SSV value of the node must be newly defined in order to determine the node which has the maximum SSV value. In this study, the sum of the SSV of the four elements around each node is used as the SSV of the node value. The previous SSVs were SSV of the element, and only the SSV of the node is used in the following description.

However, the distribution of the SSV values varies with the addition of the measurement data of strain, but the location at which the SSV value is maximum may not change. When the strain is already measured at the location where the SSV value is maximum, first, find the locations where the SSV value is local maximum and the strain is not measured, and select the next strain measurement location where the SSV value is the largest among these locations. Here, the local maximum location refers to a location where the surrounded SSV values are smaller than the center.

SSV value described above can be individually defined by the direction of the observed strain. However, as described in Chapter 2.2, z-direction strain is not used which is difficult to observe the strain value relatively. Therefore, SSV for the x-directional strain and SSV for the y-directional strain are respectively obtained. If unidirectional strain data is used, SSV in the direction in which the strain is measured is used. If both directions of strain data are used, there are two ways. The first is to use the sum of SSVs obtained in each direction. In this method, the location at which

the sum of two SSV values is the maximum is selected as the measurement location for both the next x direction strain and next y direction strain. The other is to use the SSV for the x-direction strain and the SSV for the y-direction strain respectively. In this method, the next measurement location of x-direction strain is where the x-direction SSV is the maximum, and the next measurement location of the y-direction strain is where the y-direction SSV is the maximum. Since the second method is an extension of using a unidirectional strain data, this study does not range over with the case of using a unidirectional strain data. Numerical examples of Chapter 4 obtain the results of two methods when using both directions of strain, and compare those results.

Chapter 4. Numerical Example

This section applies the sequential selection method of strain measurement location proposed in this study to a simple structure. Experiments are divided into two parts according to how the SSV in the x-direction and SSV in the y-direction are applied when selecting sequential strain measurement locations. In each part, three methods of generating sample effective thickness in Chapter 3.2 are applied. First, compare the results of the three effective thickness sample generation methods. Next, confirm the superiority of sequential strain measurement location selection method using SSV in comparison with the result of intuitive selection of strain observation locations simultaneously. Finally, use the results to conclude what is the more efficient way of applying SSV.

4.1. Structure Overview

The structure used in the experiment is a thin steel plate with a square shape when viewed from the top, as shown in Figure 4.1. The bottom edge of the left end and the right end of the steel plate are constrained by moment hinges. The information of the steel plate is as follows:

- Size of the steel plate: 2.5m × 2.5m × 0.03m
- Size of each elements: 0.15625m × 0.15625m × 0.0075m
- Number of elements for each edge: 16 × 16 × 4 elements

- Number of total elements: 1024 elements
- Number of nodes for each edge: 17 × 17 × 5 nodes
- Number of total nodes: 1445 nodes
- Stiffness of the steel plate: 200 GPa

Because of the characteristics of the steel plate, the location where strain observe is available is limited to 289 nodes at the top of the steel plate. The initial node location of observe x-direction strain and y-direction strain for select sequential strain observation location are always located at the center of the top of the steel plate.

Generally, Q8 element is used in many finite element analyses. However, the element used for finite element analysis of this numerical example is Q6 element. This is because if the finite element analysis uses the Q8 element, proposed methods have a disadvantage that the time required for each step of MCMC is too long when Bayesian updating is performed. However, only bending is important for this steel plate because of the moment hinges. Therefore, this numerical example uses the Q6 element, which has the almost same bending results as the Q8 element and can reduce the computational cost considerably.

Figure 4.2 shows the load acting on the structure. The size of the square in Figure 4.2 is the sum of the four elements. The red part is the part where the upward load is applied, and the blue part is the part where the downward load as applied. The magnitude of both upward and downward loads is 1.28MPa.

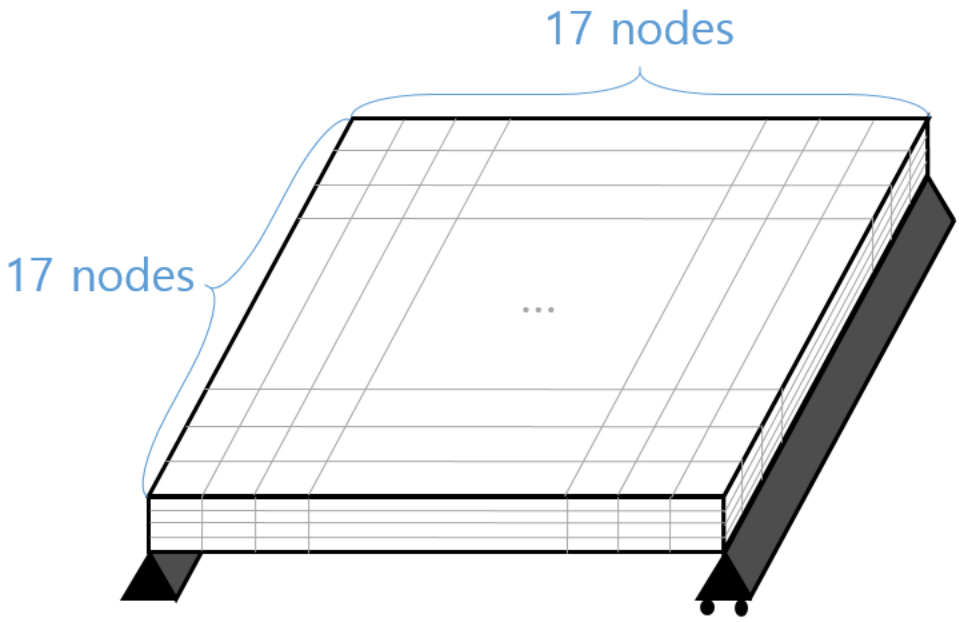

Figure 4.1. Structure to use in numerical examples: steel plate

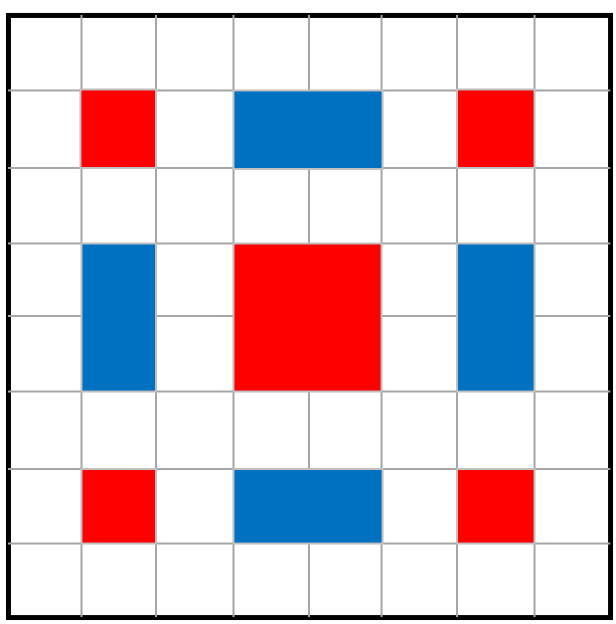

Figure 4.2. Location and direction of distributed load acting on steel plate

Simultaneous strain observation locations to comparison with results of sequential strain observation locations are shown in Figure 4.3. Two cases of simultaneous strain observation locations are selected. In the situation where only the shape of the steel plate is known, these cases use the intuitively determined location that is evenly distributed.

The covariance function used in this numerical example is not separable exponential covariance function, as follows:

$$C(\boldsymbol{x_1}, \boldsymbol{x_2}) = \exp\left(-\frac{\sqrt{(x_1 - x_2)^2 + (y_1 - y_2)^2}}{1.2}\right) \tag{4.1}$$

Because this covariance function is not separable, the finite element method using piecewise polynomial basis is used to solve the Fredholm equation of the second kind of this numerical example, as mentioned in Chapter 2.1. Eigenfunctions with 7 high-weighted eigenvalues in the linear combination are shown in Figure 4.4, and 7 eigenvalues corresponding to each eigenfunction are shown in Table 4.1. The reason why λ_2 and λ_3 have the same value is the shape of the steel plate of this example has symmetry. In this example, the order of the λ_2 and λ_3 is arbitrarily determined.

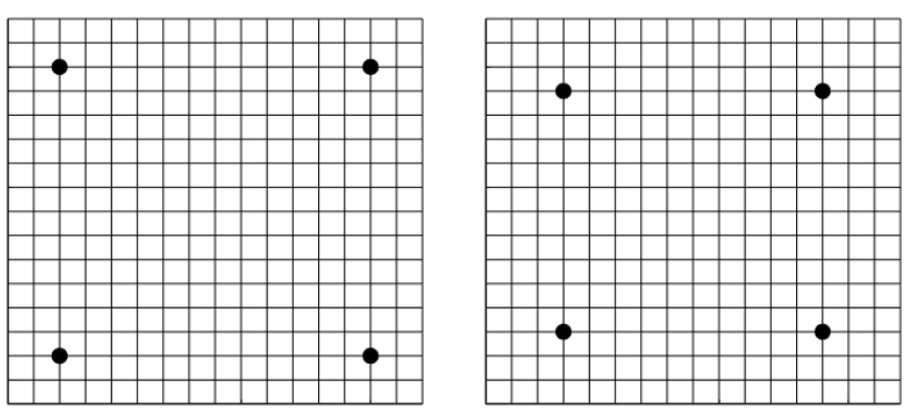

Figure 4.3. Simultaneously selected strain observation location
Left: case ‘Simultaneous 1’, Right: case ‘Simultaneous 2’

The distribution of the effective thickness used in the numerical example was the same in both examples. Figure 4.5 shows the 3D plot and contour of the effective thickness distribution. In this example, the linear combination of the eigenfunctions of the K-L expansion is used as the effective thickness distribution of the structure to omit the process of approximating the actual effective thickness distribution of the plate using K-L expansion. The number of KL random variables $\{\xi_i\}$ is set to 7, and the total number of random variables is 8, including the mean of effective thickness $\overline{w}$. Table 4.2 shows the values of the random variables of the effective thickness distribution of this numerical example, which are sampled independently from the standard normal distribution. Since the number of random variables is 8, the maximum number of strain observations was also limited to 8, including the strain of x and y directions. Because the number of measurements in the x-direction and y-direction are the same, there are four x-direction strain measurements and four y-direction strain measurements in the final result.

Random variable	λ_1	λ_2	λ_3	λ_4
Value	2.2831	0.6436	0.6436	0.2700
Random variable	λ_5	λ_6	λ_7	
Value	0.2043	0.1889	0.1132	

Table 4.1. Values of eigenvalues corresponding to each eigenfunction

Random variable	ξ_1	ξ_2	ξ_3	ξ_4
Value	0.1243	0.9271	0.7775	-0.0833
Random variable	ξ_5	ξ_6	ξ_7	$\overline{w}$
Value	0.2509	0.6391	-0.6706	0.03

Table 4.2. Values of random variables of the effective thickness

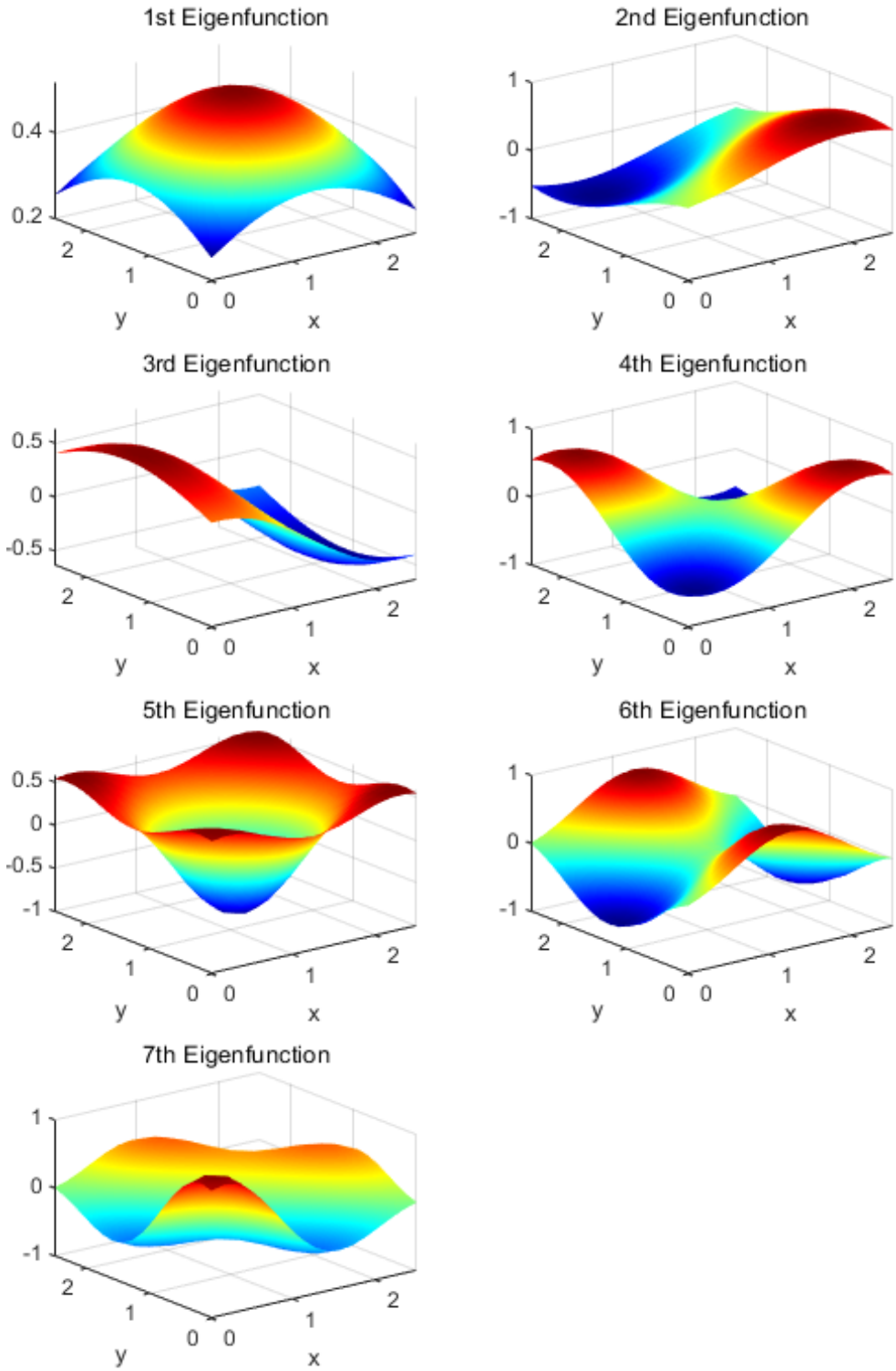

Figure 4.4. Eigenfunctions with 7 high-weighted eigenvalues

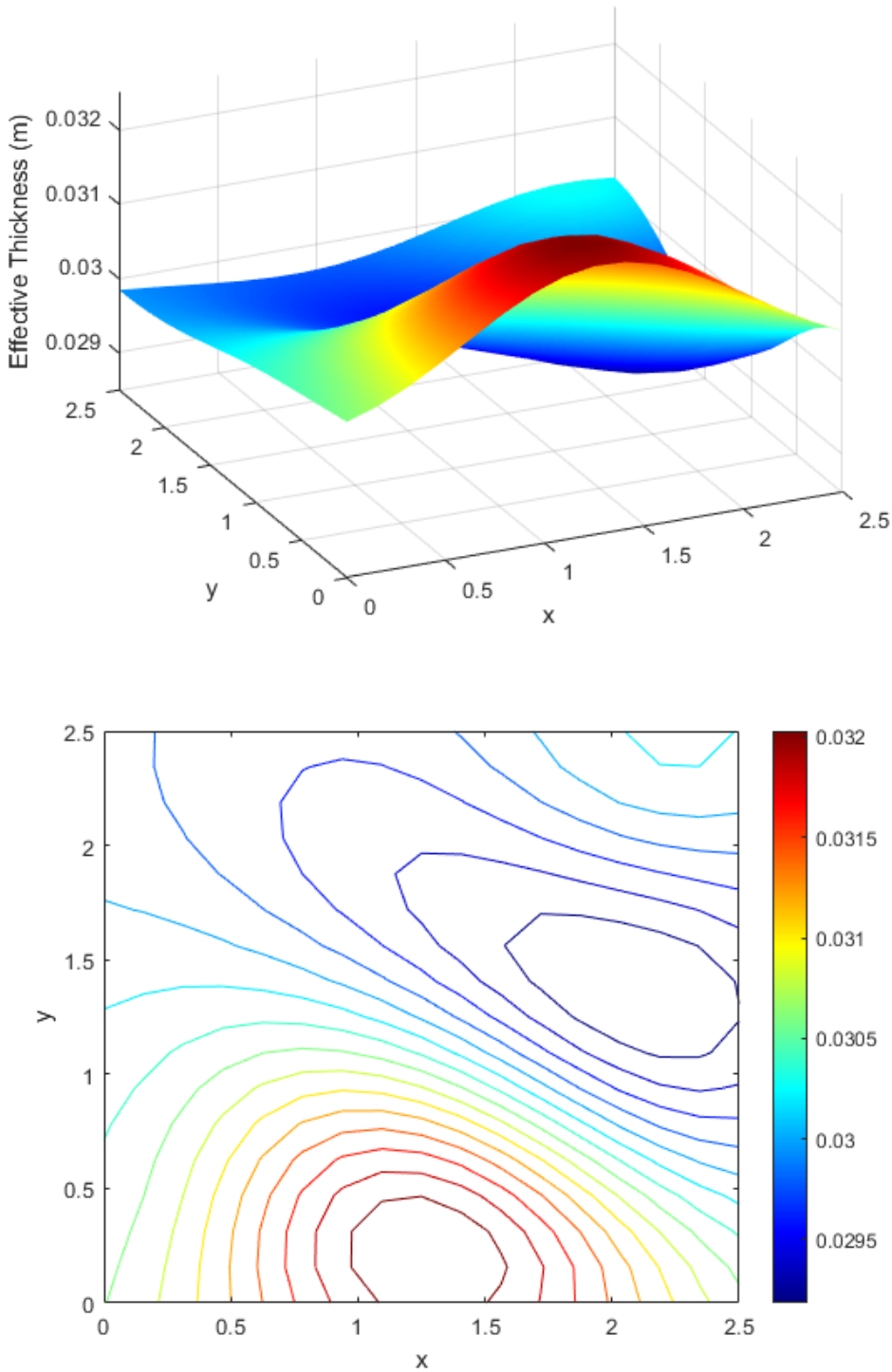

Figure 4.5. Effective thickness distribution of steel plate

Above: 3D plot, Below: contour

4.2. Numerical Example 1: Use the Sum of Two SSVs

The first numerical example is the first of two methods using both of the x and y directional strain described in Chapter 3.3. The SSV in the x direction and the SSV in the y direction are added, and measure the next strain in both directions at the location where the added SSV value is maximum. Figure 4.6 shows the variation of the sum of two SSV values in 3D plot and contour when the number of strain observations increases sequentially in the order of 2, 4, and 6 in the Scheme 1.

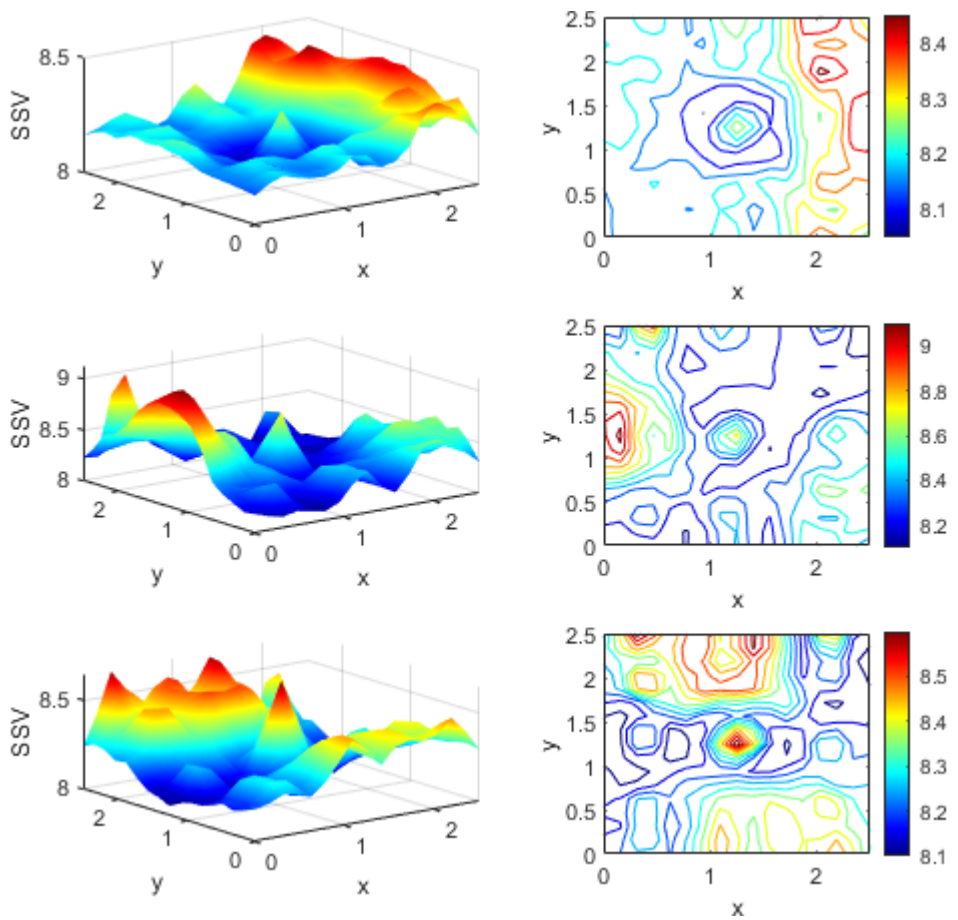

Figure 4.6. Variation of the sum of two SSV values in the Scheme 1 at Example 1 (Number of observations: 2, 4, 6 from top)

Figure 4.7 shows the sequential strain measurement locations and order in three effective thickness sample generation schemes. The black circle in the center represent the initial measurement locations, and then the strain in the x-direction and y-direction both were measured in the order of the triangle locations. The strain measurement location of each scheme showed a considerable difference, especially Scheme 2. For example, Scheme 1 and scheme 3 were not measured at the lower half of the steel plate, and Scheme 2 was measured only once at the lower half of the steel plate. In the upper half of the plate, it is intuitively inferred to have been measured evenly.

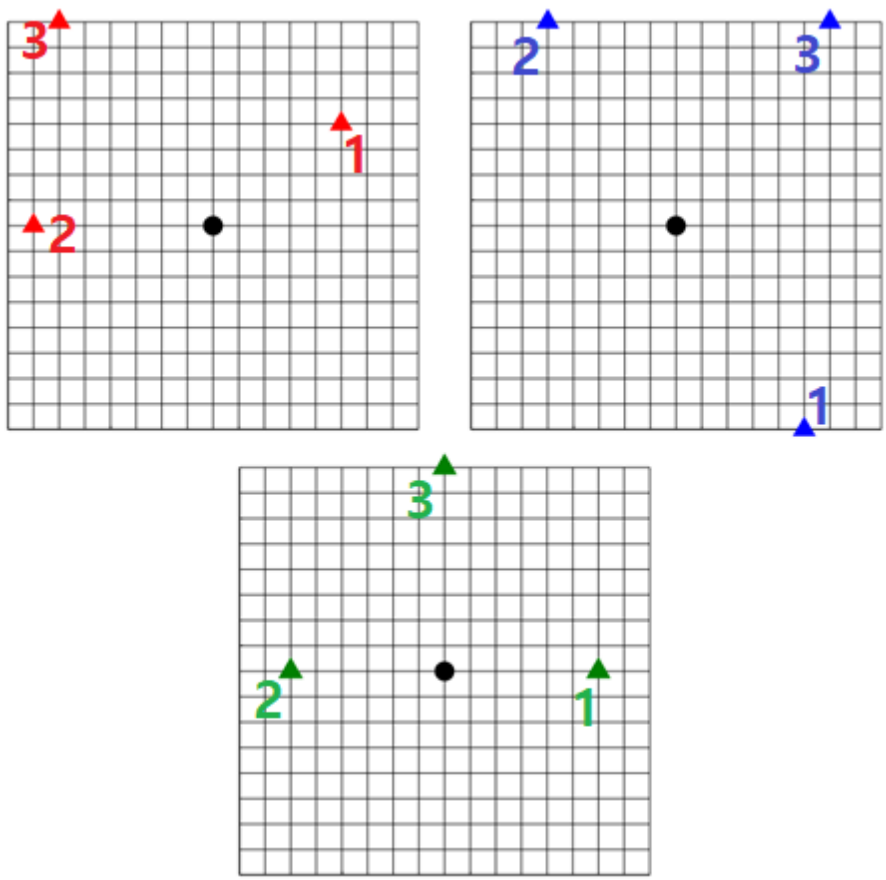

Figure 4.7. Sequential strain measurement locations and order at Example 1
Upper left: Scheme 1, Upper right: Scheme 2, Below: Scheme 3

The upper graph of Figure 4.8 shows the variation of the error between the estimated effective thickness and the actual effective thickness, and the lower graph in Figure 4.8 shows the variation of the standard deviation of the estimated effective thickness when the number of strain observation increases for each effective thickness sample generation scheme.

First, in the case of the average of the squared error, Scheme 2 showed the smallest error at the end. However, before the number of measurements reached the target value, the scheme with the smallest error varied. Furthermore, in the case of the average of standard deviation, the standard deviation of Scheme 1 was the smallest regardless of the number of sensors. In addition, the standard deviation increased slightly when the number of sensors is increased in Scheme 3. This is because the number of random variables to be determined is greater than the number of strain measurements, therefore ill-posedness has occurred. This situation did not occur when the number of strain measurement reaches the target value.

Figure 4.9 compares the final errors and standard deviations for the case of selecting strain measurement locations sequentially and simultaneously. As a result, there was no significant difference in error and standard deviation between two cases.

In conclusion, the efficiency of Scheme 1 in terms of error and Scheme 2 in terms of standard deviation is relatively good when the x-direction and y-direction strain are measured at the same location. However, there was no significant effect compared with the case that the observation locations are selected intuitively and simultaneously. In addition, errors and standard deviations before reaching the final number of sensors were not significant for comparison due to ill-posedness. As a result, Example 1 is an inefficient sequential measurement location selection method.

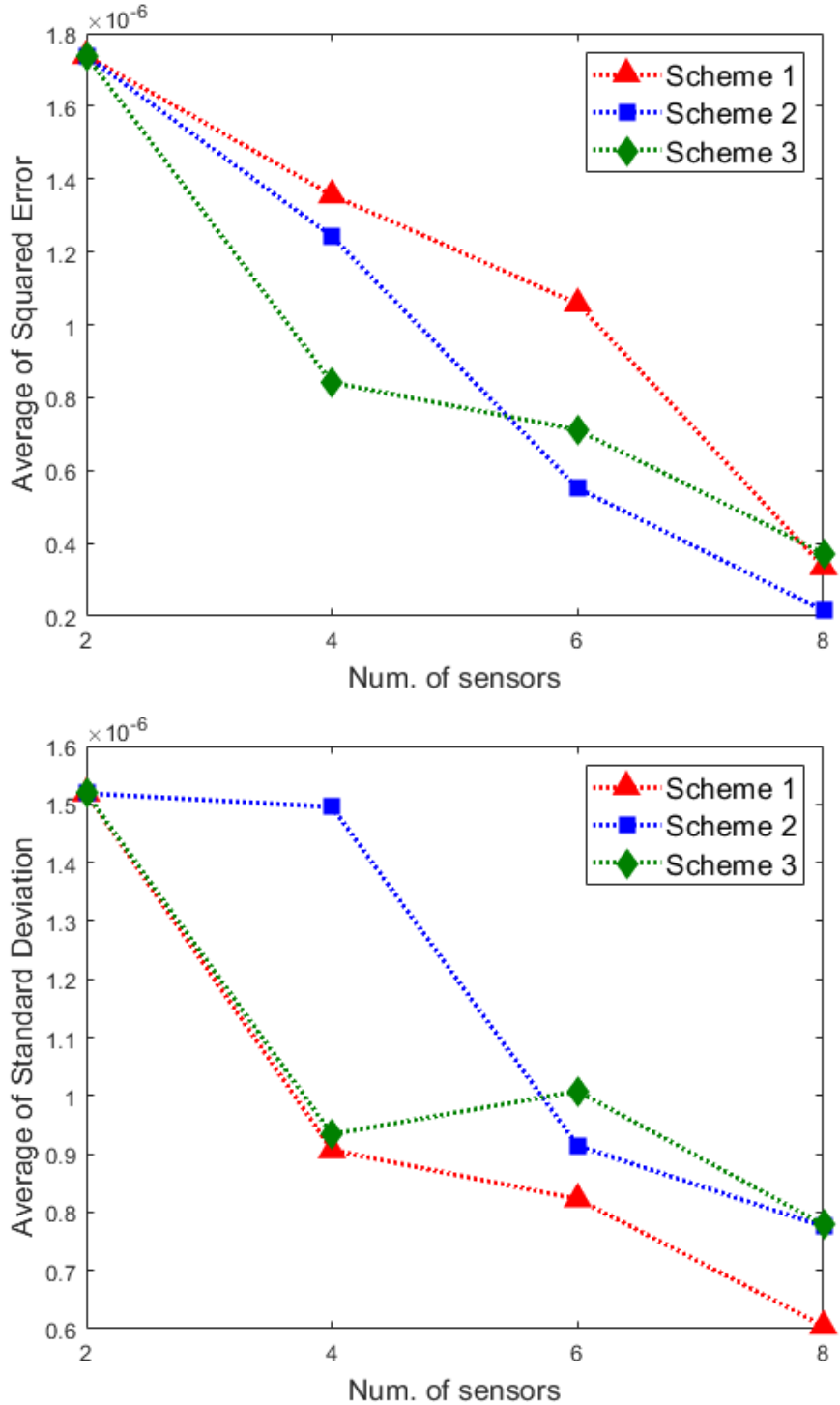

Figure 4.8. Above: The error between the estimated and actual effective thickness at the Example 1, Below: The standard deviation of the estimated effective thickness at the Example 1

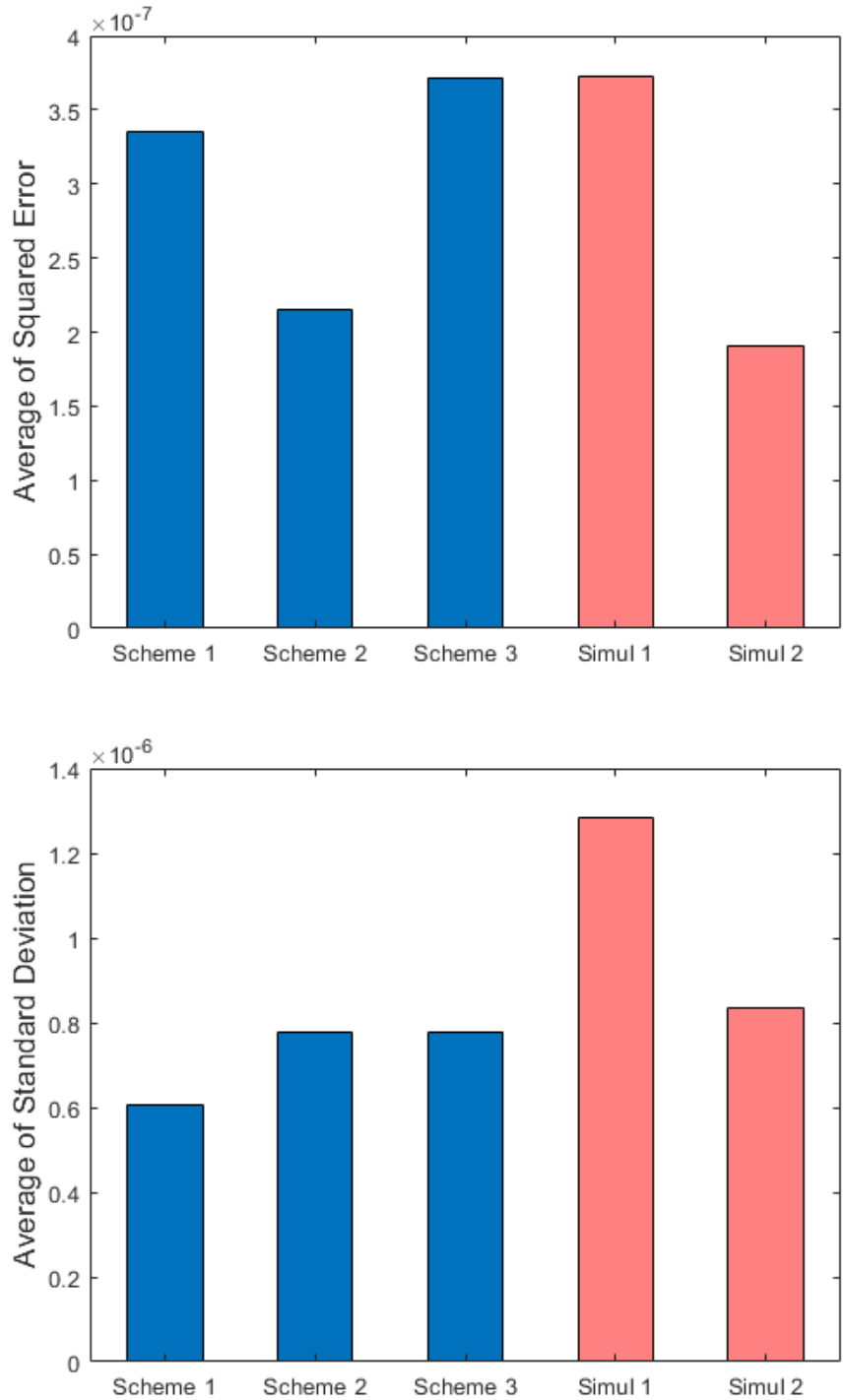

Figure 4.9. Compare for the selecting strain measurement locations sequentially and simultaneously at Example 1, Above: error, Below: effective thickness

4.3. Numerical Example 2: Use Two SSVs Respectively

The second numerical example is the second of two methods using both of the x and y directional strain described in Chapter 3.3. Measure the next x-direction strain at the location where the x-direction SSV is the maximum, and same to the y-direction. Figure 4.10 shows the variation of the x-direction SSV values in 3D plot and contour when the number of strain observations increases sequentially in the order of 2, 4, and 6 in the Scheme 2, and Figure 4.11 shows the variation of the y-direction SSV values in 3D plot and contour.

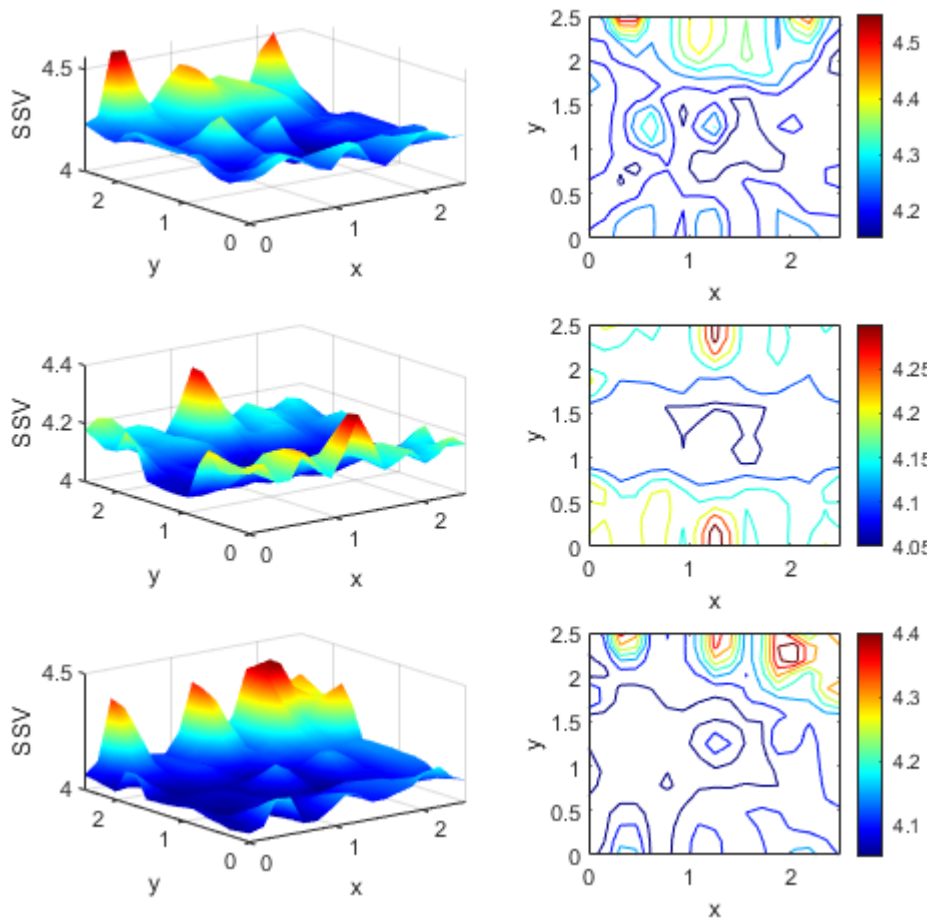

Figure 4.10. Variation of the x-direction SSV values in the Scheme 1 at example 2 (Number of observations: 2, 4, 6 from top)

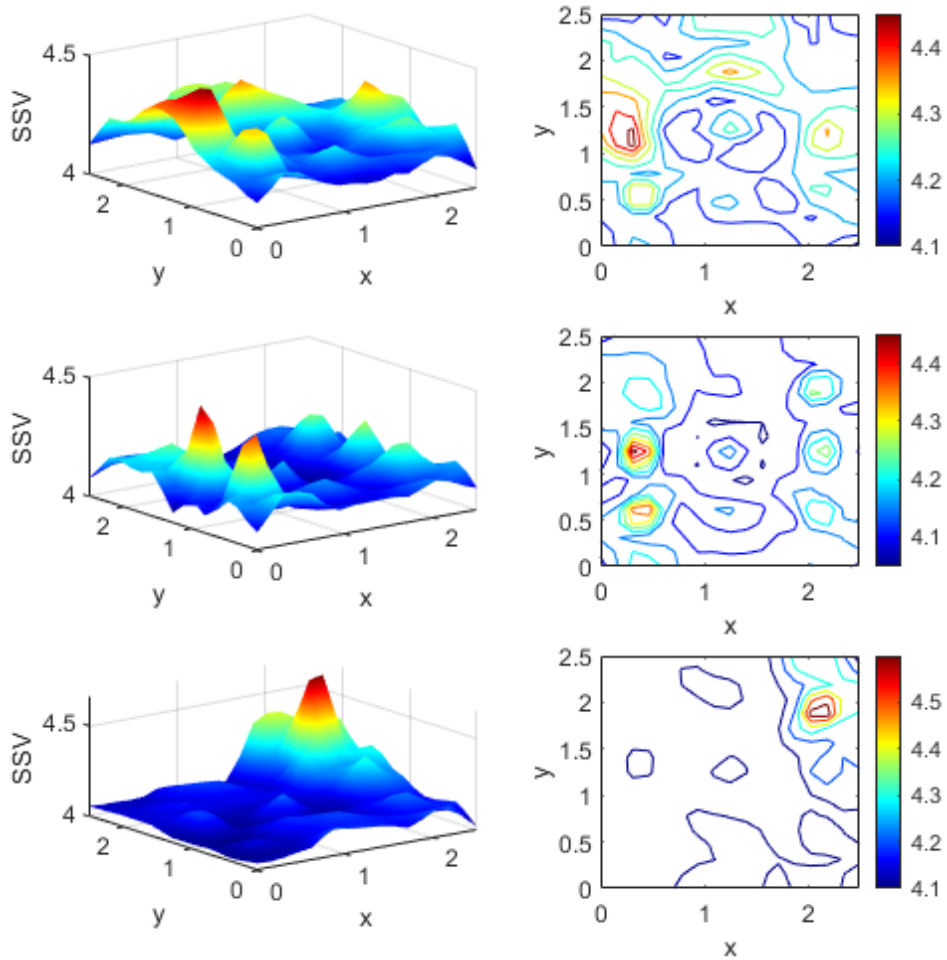

Figure 4.11. Variation of the y-direction SSV values in the Scheme 1 at example 2 (Number of observations: 2, 4, 6 from top)

Figure 4.12 shows the sequential strain measurement locations and order in three effective thickness sample generation schemes. The black circles in the center represent the initial measurement locations, and then strains in the x-direction were measured in the order of the triangle locations, and strains in the y-direction were measured in the order of the inverted triangle locations. Unlike Example 1 which measures both strains in two directions at the same location using the result of adding two SSVs, it can be intuitively inferred that strain measurement locations were distributed evenly in all three schemes.

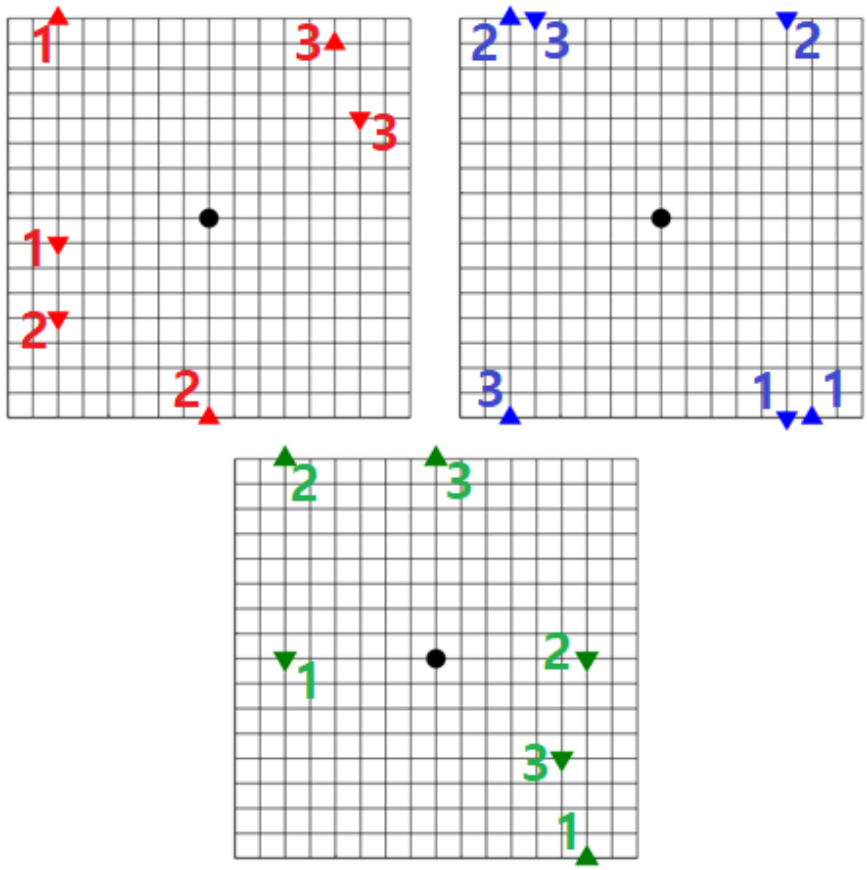

Figure 4.12. Sequential strain measurement locations and order at example 2
Upper left: Scheme 1, Upper right: Scheme 2, Below: Scheme 3

The upper graph in Figure 4.13 shows the variation of the error between the estimated effective thickness, and the lower graph in Figure 4.13 shows the actual effective thickness and the variation of the standard deviation of the estimated effective thickness when the number of strain observation increases for each effective thickness sample generation scheme. Unlike Example 1, Scheme 3 gives the best results regardless of the number of strain measurements in both error and standard deviation. In addition, standard deviations also increase slightly when the number of sensors is increased in Scheme 1 and Scheme 2. This situation is also presumed by the ill-posedness.

Figure 4.14 compares the final errors and standard deviations for the case of selecting strain measurement locations sequentially and simultaneously. In the case of the average of squared errors, Scheme 1 and Scheme 3 showed a significant decrease in error when compared to the Simultaneous 2 case which has a smaller error among the two simultaneous cases. Numerically, Scheme 1 showed an error reduction of about 58%, and Scheme 3 showed an error reduction of about 62% compared to Simultaneous 2 case. On the other hand, Scheme 2 showed an error similar to Simultaneous 2 case. This result was different from Chapter 3.2.2 which Scheme 2 is more accurate. It can be deduced that the disadvantage of cannot considering correlation of effective thickness of adjacent nodes has a great influence.

Average of standard deviation showed a similar tendency. Scheme 1 showed a standard deviation reduction of about 38%, and Scheme 3 showed a standard deviation reduction of about 47% compared to Simultaneous 2 case. On the other hand, standard deviation of Scheme 2 is slightly larger than the simultaneous case, therefore the accuracy is also poor.

In conclusion, the accuracy of Scheme 3 was highest for both error and standard deviation when x-direction strain measurement and y-direction strain measurement were performed at different locations, and accuracy of Scheme 1 was also high. In addition, it shows that there is a significant effect in the accuracy of selecting the sequential measurement location using SSV because it shows a significant difference compared with the case when the observation location is intuitively selected. This also means that determining the x-direction and y-direction strain measurement locations respectively are more effective than determining both direction strain measurement at the same location.

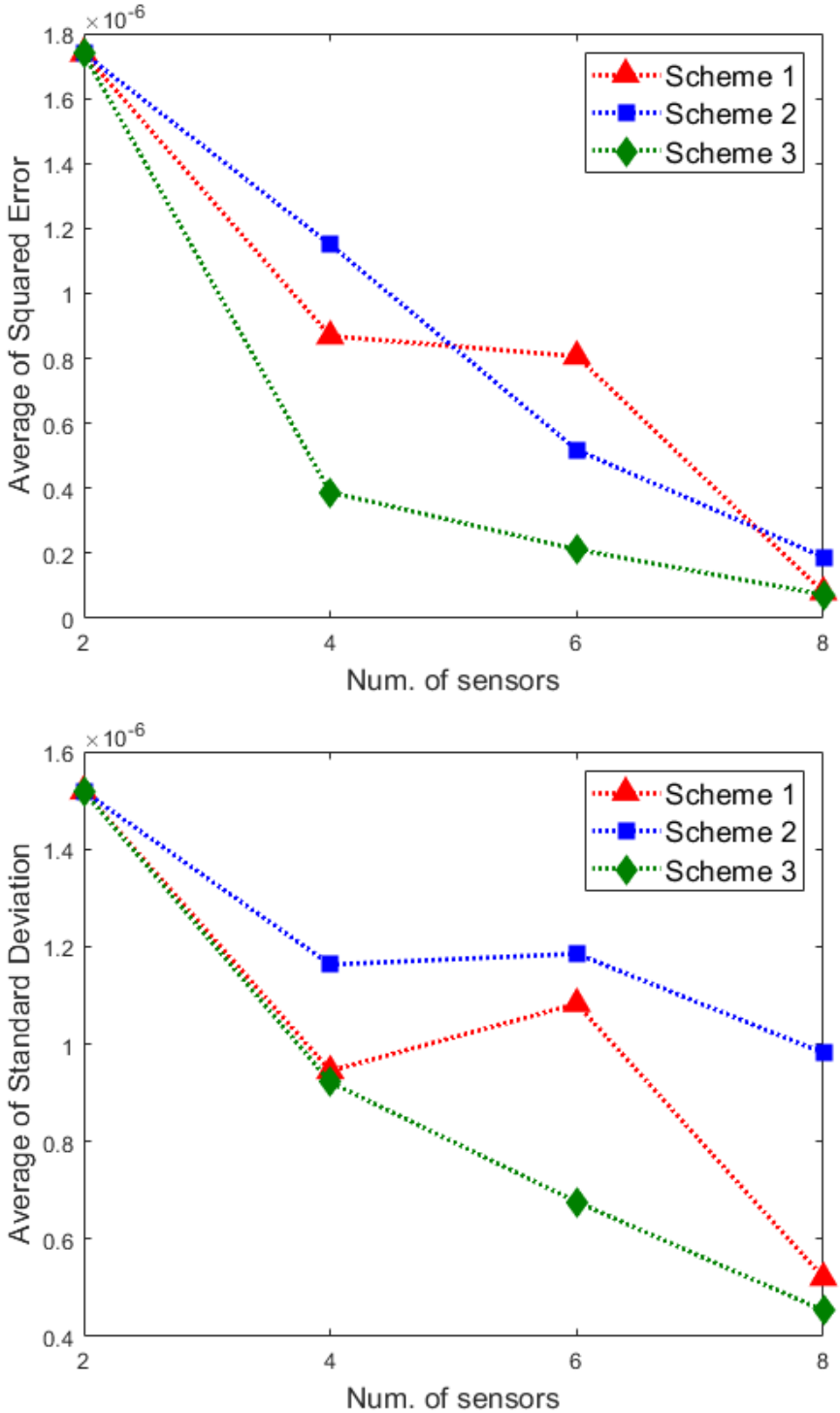

Figure 4.13. Above: The error between the estimated and actual effective thickness at the example 2, Below: The standard deviation of the estimated effective thickness at the example 2

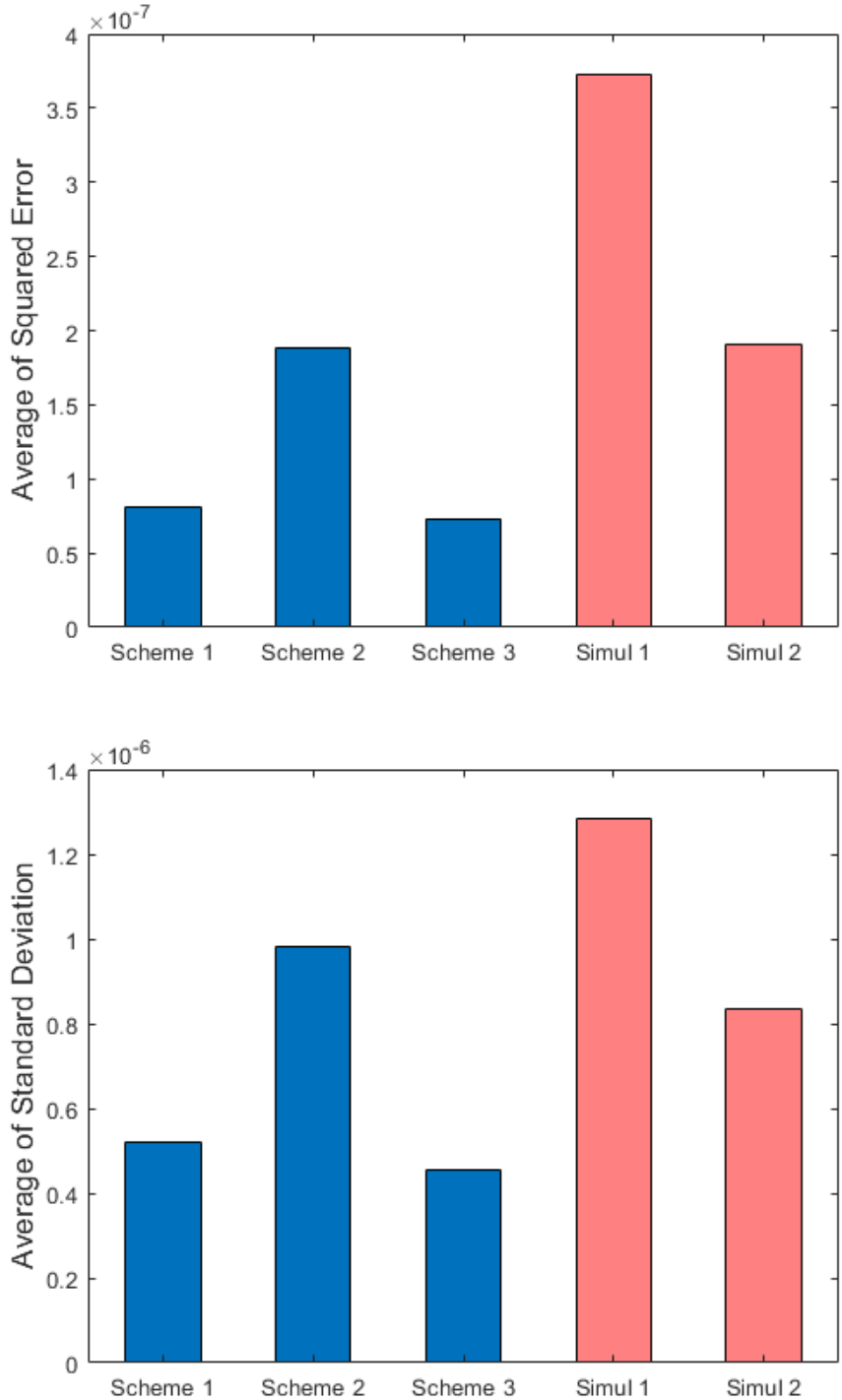

Figure 4.14. Compare for the selecting strain measurement locations sequentially and simultaneously at example 2, Above: error, Below: effective thickness

Chapter 5. Conclusion

When selecting strain measurement locations for system identification, large errors and deviations could occur when measurement locations are selected based on intuition or engineering judgement and simultaneously using only the shape of the structure and the applied load without prior information. Alternatively, if the strain measurement locations are selected sequentially, it is possible to estimate effective thickness temporarily. Using the temporarily estimated effective thickness, it is possible to select the next measurement location that is expected to improve estimation accuracy.

In this study, the effective thickness and its confidence interval of the structure are indirectly estimated by using the given displacement measurement values, and the methods of sequentially determining additional observation locations are proposed to effectively reduce the error and standard deviation of the effective thickness estimation. It is confirmed that the finally estimated effective thickness distribution with selected strain locations by the sequential strain observation location selection method proposed in this study has smaller errors and standard deviations when compared with the selected strain measurement locations without estimated effective thickness distribution.

Sequentially selected measurement locations using suggested schemes have higher accuracy than simultaneously selected measurement locations for estimate effective thickness. Based on this method, it will be possible to implement an initial

inspection of a large number of old structures which has the possibility of overall deterioration with a limited budget.

Future research topics are identified as follows: first, if the number of possible observation is small, the selection of the sequential observation locations will be greatly affected by the initial location. Therefore, I want to study the selection of the initial observation location according to the applied load. In addition, because of the present SSV value may show a large value at the location where the strain is already observed, I will propose a new value that solves this problem. Lastly, since it takes a long time to select one measurement location at a time, it is desirable to select multiple measurement locations simultaneously while maintaining the estimation accuracy.

References

Betz, W., Papaioannou, I., & Straub, D. (2014). Numerical methods for the discretization of random fields by means of the Karhunen–Loève expansion. *Computer Methods In Applied Mechanics And Engineering*, *271*, 109-129.

Dickinson, B., Fettweis, A., & Massey, J. (1993). *Markov Chains and Stochastic Stability*. London: Springer London.

Ghanem, R., & Spanos, P. (1991). *Stochastic Finite Elements: A Spectral Approach*. New York, NY: Springer New York.

Ginsbourger, D., Le Riche, R., Carraro, L. (2010). Kriging is well-suited to parallelize optimization, In Tenne, Y., Goh, C.K. (eds.), *Computational Intelligence in Expensive Optimization Problems*. Adaptation Learning and Optimization, 131-162.

Springer, Heidelberg. (2010) Goodman, J., & Weare, J. (2010). Ensemble samplers with affine invariance. *Communications In Applied Mathematics And Computational Science*, *5*(1), 65-80.

Huang, S., Quek, S., & Phoon, K. (2001). Convergence study of the truncated Karhunen–Loeve expansion for simulation of stochastic processes. *International Journal For Numerical Methods In Engineering*, *52*(9), 1029-1043.

Jones, D., Schonlau, M., & Welch, W. (1998). Efficient Global Optimization of

Expensive Black-Box Functions. *Journal Of Global Optimization*, *13*(4), 455-492.

Karhunen, K. (1947). Ueber lineare Methoden in der Wahrscheinlichkeitsrechnung. *Annales Academiae Scientiarum Fennicae. Series A. 1, Mathematica-Physica*, *37*.

Kleijnen, J., van Beers, W., & van Nieuwenhuyse, I. (2011). Expected improvement in efficient global optimization through bootstrapped kriging. *Journal Of Global Optimization*, *54*(1), 59-73.

Kučerová, A., & Sýkora, J. (2013). Uncertainty updating in the description of coupled heat and moisture transport in heterogeneous materials. *Applied Mathematics And Computation*, *219*(13), 7252-7261.

Lee, S., & Song, J. (2017). System Identification of Spatial Distribution of Structural Parameters Using Modified Transitional Markov Chain Monte Carlo Method. *Journal Of Engineering Mechanics*, *143*(9), 04017099.

Li, J. (2015). A note on the Karhunen–Loève expansions for infinite-dimensional Bayesian inverse problems. *Statistics & Probability Letters*, *106*, 1-4.

Loève, M. (1963). *Probability theory*. Princeton, N.J.: Van Nostrand.

Matthias, S. (1997). Computer Experiments and Global Optimization (PhD dissertation). University of Waterloo, Ontario, Canada.

Mondal, A., Mallick, B., Efendiev, Y., & Datta-Gupta, A. (2014). Bayesian Uncertainty Quantification for Subsurface Inversion Using a Multiscale Hierarchical Model. *Technometrics*, *56*(3), 381-392.

Rasmussen, C., & Williams, C. (2006). *Gaussian processes for machine learning*. Cambridge, Mass.: MIT Press.

V. Picheny, D. Ginsbourger, & Y. Richet (2010). Noisy expected improvement and on-line computation time allocation for the optimization of simulators with tunable fidelity, *2nd International Conference on Engineering Optimization*, September 6-9, Lisbon, Portugal.

Yi, S., & Song, J. (2018). Particle Filter Based Monitoring and Prediction of Spatiotemporal Corrosion Using Successive Measurements of Structural Responses. *Sensors*, *18*(11), 3909.

초 록

구조물은 사용 기간이 오래될수록 자연히 열화되므로, 구조물 붕괴 등의 사고를 미연에 방지하기 위해서는 구조물의 열화 정도를 정확히 파악하는 것이 필수적이다. 그러나, 열화 정도를 파악할 수 있는 유효 두께 등의 수치들은 직접 측정이 힘든 경우가 많으므로 하중 재하 시험 등에서 얻을 수 있는 변형도나 변위 등의 역학적인 관측값을 이용하여 간접적으로 추정해야 한다. 이 때, 외부 요인으로 인하여 가능한 직접 측정 위치 개수가 한정되어 있다면, 한정된 개수의 관측값 하에서 가능한 간접 추정 정확도를 향상시킬 수 있는 직접 측정 위치 선정을 필요로 한다.

본 연구에서는 변형도 측정 위치 개수가 제한되어 있을 때 구조물의 유효두께 간접 추정의 정확도를 향상시키기 위해 순차적 측정 위치 최적화 방식을 제시한다. 먼저 구조물의 유효 두께 분포를 Karhunen-Loève 모델을 사용하여 근사적으로 표현한 뒤, 마르코프 연쇄 몬테카를로를 사용하는 베이즈 추론을 기반으로 한 역해석을 수행하여 주어진 변형도 측정값 하에서 구조물 전체의 유효두께의 추정값과 편차를 추정한다. 다음으로 추정된 유효두께의 추정값과 편차를 이용하여 관측 위치를 선정하는 세 가지의 관측 위치 선정 방법을 제안한다. 마지막으로, 제안된 방법들을 실제로 구조물에 적용해서 관측

위치 선정 방법들의 정확도를 비교하고, 또한 동시에 관측 위치를 선정한 경우와 정확도를 비교한다.

제안된 방법들을 통하여 유효두께 추정값의 정확도를 효과적으로 향상시킬 수 있는 다음 변위 측정 위치를 결정할 수 있으며, 이를 통해 한정된 관측 위치 개수 하 에서 유효두께 추정의 정확도를 최대화할 수 있다. 제안된 방식은 유효두께뿐만 아니라, 샘플링을 통하여 간접적으로 추론해낼 수 있는 다양한 구조물 열화 관련 물성치 추정의 정확도 향상에도 적용될 수 있을 것으로 기대된다.

주요어: 구조물 열화, 유효두께, Karhunen-Loève 모델, 마르코프 연쇄 몬테카를로, 베이즈 추론, 역해석

학번: 2017-24757